2. Tateno C, Yoshizane Y, Saitou N, et al. Near completely humanized liver in mice shows human-type metabolic responses to drugs. Am J Pathol 2004;165:901–912.

3. Katoh M, Matsui T, Okamura H, et al. Expression of human phase II enzymes in chimeric mice with humanized liver. Drug Metab Dispos 2005;33:1333–1340.

4. Nishimura M, Yoshitsugu H, Yokoi T, et al. Evaluation of mRNA expression of human drug-metabolising enzymes and transporters in chimeric mouse with humanized liver. Xenobiotica 2005;35:877–890.

5. Shi J, Fujieda H, Kokubo Y, et al. Apoptosis of neutrophils and their elimination by Kupffer cells in rat liver. Hepatology 1996;24:1256–1263.

6. Warren A, Le Couteur DG, Fraser R, et al. T lymphocytes interact with hepatocytes through fenestrations in murine liver sinusoidal endothelial cells. Hepatology 2006;44:1182–1190.

7. Sato Y, Yamada H, Iwasaki K, et al. Human hepatocytes can repopulate mouse liver: histopathology of the liver in human hepatocyte-transplanted chimeric mice and toxicologic responses to acetaminophen. Toxicol Pathol 2008;36:581–591.

8. Meuleman P, Libbrecht L, De Vos R, et al. Morphological and biochemical characterization of a human liver in a uPA-SCID mouse chimera. Hepatology 2005;41:847–856.

9. Nonaka H, Tanaka M, Suzuki K, et al. Development of murine hepatic sinusoidal endothelial cells characterized by the expression of hyaluronan receptors. Dev Dyn 2007;236:2258–2267.

10. Katayama S, Tateno C, Asahara T, et al. Size-dependent in vivo growth potential of adult rat hepatocytes. Am J Pathol 2001;158:97–105.

11. Ban D, Kudo A, Sui S, et al. Decreased Mrp2-dependent bile flow in the after-warm ischemic rat liver. J Surg Res 2009;153:310–316.

12. Mabuchi A, Wake K, Marlini M, et al. Protection by glycyrrhizin against warm ischemia-reperfusion-induced cellular injury and derangement of the microcirculatory blood flow in the rat liver. Microcirculation 2009;16:364–376.

13. Wisse E, Braet F, Duimel H, et al. Fixation methods for electron microscopy of human and other liver. World J Gastroenterol 2010;16:2851–2866.

14. Seglen PO. Preparation of isolated rat liver cells. Methods Cell Biol 1976;13:29–83.

15. Bolstad BM, Irizarry RA, Astrand M, et al. A comparison of normalization methods for high density oligonucleotide array data based on variance and bias. Bioinformatics 2003;19:185–193.

16. Eisen MB, Spellman PT, Brown PO, et al. Cluster analysis and display of genome-wide expression patterns. Proc Natl Acad Sci USA 1988;95:14863–14868.

17. Tateno C, Kataoka M, Utoh R, et al. Growth hormone-dependent pathogenesis of human hepatic steatosis in a novel mouse model bearing a human hepatocyte-repopulated liver. Endocrinology 2011;152:1479–1491.

18. Asahina K, Sato H, Yamasaki C, et al. Pleiotrophin/HB-GAM as a mitogen of rat hepatocytes and its role in regeneration and development of liver. Am J Pathol 2002;160:2191–2205.

19. Benjamini Y, Hochberg Y. Controlling the false discovery rate: a practical and powerful approach to multiple testing. J Roy Statist Soc Ser B 1995;57:289–300.

20. Utoh R, Tateno C, Kataoka M, et al. Hepatic hyperplasia associated with discordant xenogeneic parenchymal-nonparenchymal interactions in human hepatocyte-repopulated mice. Am J Pathol 2010;177:654–665.

21. Michael L. Laboratory Medicine: The Diagnosis in the Clinical Laboratory, New York, 2010.

22. Jensen FS, Skovgaard LT, Viby-Mogensen J. Identification of human plasma cholinesterase variants in 6,688 individuals using biochemical analysis. Acta Anaesthesiol Scand 1995;39:157–162.

23. Porter RK, Brand MD. Causes of differences in respiration rate of hepatocytes from mammals of different body mass. Am J Physiol 1995;269:R1213–R1224.

24. Maeno H, Ono T, Dhar DK, et al. Expression of hypoxia inducible factor-1alpha during liver regeneration induced by partial hepatectomy in rats. Liver Int 2005;25:1002–1009.

25. Tomoyori T, Ogawa K, Mori M, et al. Ultrastructural changes in the bile canaliculi and the lateral surfaces of rat hepatocytes during restorative proliferation. Virchows Arch B Cell Pathol Incl Mol Pathol 1983;42:201–211.

26. Souza SC, Frick GP, Wang X, et al. A single arginine residue determines species specificity of the human growth hormone receptor. Proc Natl Acad Sci USA 1995;92:959–963.

27. Masumoto N, Tateno C, Tachibana A, et al. GH enhances proliferation of h-heps grafted into immunodeficient mice with damaged liver. J Endoclinol 2007;194:529–537.

28. Sandgren EP, Palmiter RD, Heckel JL, et al. Complete hepatic regeneration after somatic deletion of an albumin-plasminogen activator transgene. Cell 1991;66:245–256.

29. Dinchuk J, Hart J, Gonzalez G, et al. Remodelling of lipoproteins in transgenic mice expressing human cholesteryl ester transfer protein. Biochim Biophys Acta 1995;1255:301–310.

Transplantation of Engineered Chimeric Liver With Autologous Hepatocytes and Xenobiotic Scaffold

Toshiyuki Hata, MD,*† Shinji Uemoto, MD, PhD,* Yasuhiro Fujimoto, MD, PhD,* Takashi Murakami, MD, PhD,‡ Chise Tateno, PhD,§ Katsutoshi Yoshizato, PhD,§ and Eiji Kobayashi, MD, PhD||

Objective: Generation of human livers in pigs might improve the serious shortage of grafts for human liver transplantation, and enable liver transplantation without the need for deceased or living donors. We developed a chimeric liver (CL) by repopulation of rat hepatocytes in a mouse and successfully transplanted it into a rat recipient with vessel reconstruction. This study was designed to investigate the feasibility of CL for supporting the recipient after auxiliary liver grafting.

Methods: Hepatocytes from luciferase transgenic or luciferase/LacZ double-transgenic rats were transplanted into 20- to 30-day-old urokinase-type plasminogen activator/severe-combined immunodeficiency (uPA/SCID) mice (n = 40) to create CLs with rat-origin hepatocytes. After replacement of mouse hepatocytes with those from rats, the CLs were transplanted into wild-type Lewis (n = 30) and analbuminemia (n = 10) rats, followed by immunosuppression using tacrolimus (TAC) with/without cyclophosphamide (CPA) or no immunosuppression. Organ viability was traced by in vivo bioimaging and Doppler ultrasonography in the recipient rats for 4 to 6 months. Rat albumin production was also evaluated in the analbuminemia rats for 4 months. In addition, histological analyses including Ki67 proliferation staining were performed in some recipients.

Results: Both immunosuppressive protocols significantly improved graft survival and histological rejection of CLs as compared to the nonimmunosuppressed group. Although rat albumin production was maintained in the recipients for 4 months after transplantation, ultrasonography revealed patent circulation in the grafts for 6 months. Ki67 staining analysis also revealed the regenerative potential of CLs after a hepatectomy of the host native liver, whereas immune reactions still remained in the mouse-origin structures.

Conclusions: This is the first report showing that engineered CLs have potential as alternative grafts to replace the use of grafts from human donors.

Keywords: alternative organ graft, auxiliary liver transplantation, chimeric liver, engineered organ, liver transplantation

(Ann Surg 2013;257: 542–547)

Liver transplantation is currently regarded as the most effective treatment for end-stage liver diseases. Because the worldwide graft shortage remains unresolved,[1,2] engineered organs are anticipated as alternative grafts to fill the scarcity and ultimately replace those from deceased and living donors. Although regenerative technology has already developed various kinds of regenerative cells and tissues,[3,4] they are still insufficient to cure patients with end-stage liver diseases because of the absence of complicated functions and limited volume. Therefore, a regenerative liver graft for use as an "organ" is required. To achieve an appropriate 3-dimensional structure and differentiation to specific tissues in a single organ, application of native organs as scaffolds has been reported as a possible solution.[5–7] Recent advances in genetic manipulation of animals such as pigs have produced transgenic animals with a lower risk of xenorejection.[8,9] Thus, using their native organogenetic potentials, development of engineered liver "organs" is expected.[10] In such a protocol, human hepatocytes are transplanted to a transgenic pig to replace its native hepatocytes, resulting in development of a chimeric liver (CL) with human parenchyma and swine nonparenchymal components, including vessels, bile ducts, and other connecting tissues. However, it is unclear whether such engineered CLs can be transplanted into recipients, or whether they can maintain their organ structures and functions after transplantation. In this study, we developed a rodent model of chimeric liver transplantation to investigate its feasibility (Fig. 1A). We used mice and rats as substitutes for transgenic pigs and humans, respectively, and created CLs in transgenic mice using hepatocytes derived from transgenic rats. After chimeric liver transplantation into rat recipients with vessel reconstruction, we examined the long-term viability and functions of the transplanted CL grafts.

MATERIALS AND METHODS

Animals

All mice and rats were housed in a temperature-controlled environment under a 12-hour light-dark cycle with free access to water and standard rodent chow diet. Male and female albumin enhancer-/promoter-driven urokinase-type plasminogen activator/severe-combined immunodeficiency (uPA/SCID) mice (Phoenixbio Co, Ltd, Japan) (n = 40), which express and accumulate urokinase-type plasminogen specifically in native hepatocytes, resulting in liver disease,[11,12] were used as the scaffolds for CL regeneration. Male luciferase transgenic Lewis (Luc-LEW) (MHC haplotype; RT1^l)[13] (n = 2), and female luciferase and LacZ double-transgenic Lewis (Luc/LacZ-LEW) (RT1^l) rats[14] (n = 1) were used as hepatocyte donors. Male wild-LEW rats (RT1^l) (Charles River Japan, Japan) (n = 30) and male Nagase analbuminemia rats (RT1^a)[15] (Japan SLC, Japan) (n = 10) were used as the recipients of chimeric liver transplantation. All experiments in this study were performed in accordance with the Jichi Medical University Guide for Laboratory Animals after approval by the ethics committee of PhoenixBio Co, Ltd.

Generation of CLs

Isolated hepatocytes were obtained from 10-week-old Luc-LEW and Luc/LacZ LEW rats using a standard 2-step collagenase
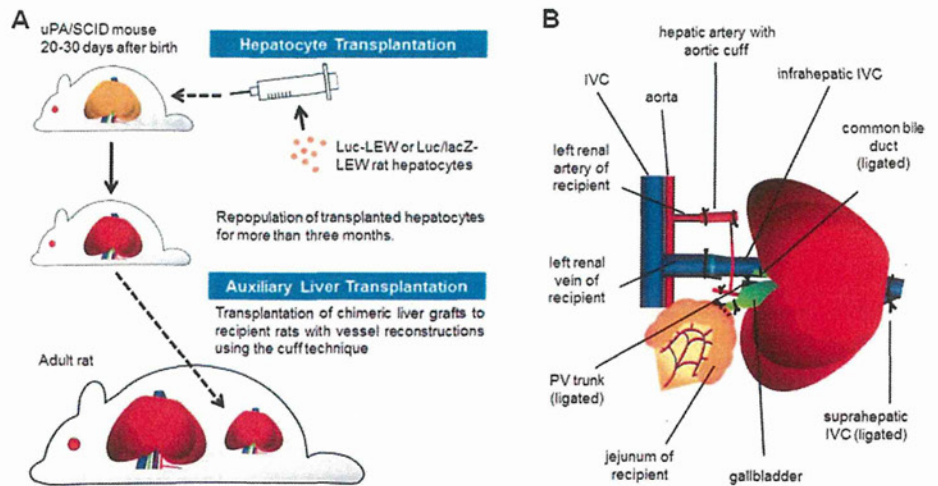
FIGURE 1. A, Experimental protocol used for Chimeric liver transplantation. B, Schema of engraftment of CL into recipient rat.

perfusion method.[16] Collagenase (75 mg/body) (COLLAGENASE S-1; Nitta-gelatin, Japan) was perfused through the portal vein, then 5.0 $\times 10^5$ hepatocytes were transplanted into 20- to 30-day-old uPA/SCID mice, as previously reported.[12] These mice were kept for 3 months to obtain CLs with satisfactory size (mean $\pm$ SEM, 1.69 ± 0.04 g) and chimerism.

Harvesting of CLs

The CLs were harvested from uPA/SCID mice along with the hepatic artery with the aortic cuff and infrahepatic inferior vena cava. The portal vein trunk, common bile duct, and suprahepatic inferior vena cava were ligated. After systemic injection of 300 U of heparin sodium (Novo-Heparin; Mochida, Japan), the graft was harvested and cryo-preserved in 0.9% saline. A 10-mm plastic tube (22G SurfloR, IV catheter; Terumo, Japan) was inserted into the gallbladder, and a plastic cuff (18G SurfloR) was installed onto the end of the infrahepatic inferior vena cava.

Auxiliary Liver Transplantation of CLs

The CLs were engrafted in an auxiliary manner with vessel reconstruction using a cuff technique, as we previously reported.[17] In brief, after a simple left nephrectomy, a plastic cuff (22G SurfloR) was installed on the end of the recipient left renal artery. The graft hepatic artery and infrahepatic inferior vena cava were anastomosed to the recipient left renal artery and vein, respectively (see Video and Figure, Supplemental Digital Contents 1 and 2, demonstrating reperfusion of graft, available at http://links.lww.com/SLA/A254 and http://links.lww.com/SLA/A256, respectively). The graft gallbladder was connected to the recipient jejunum (Fig. 1B) and the recipient liver was left intact. There were no significant differences regarding any of the parameters for the animals and surgical procedures (data not shown). Recipient rats that died within 24 hours after chimeric liver transplantation or showed no luminescent signals on day 1 were excluded from postoperative analyses.

PostTransplant Treatment

Solid immunosuppressive protocols with tacrolimus (TAC) for T cell–mediated rejection and cyclophosphamide (CPA) for antibody-mediated rejection were used. The LEW rat recipients were treated with one of the following protocols: daily tacrolimus [TAC (+)CPA (−)] (n = 15), daily tacrolimus and cyclophosphamide pre-treatment [TAC (+)CPA(+)] (n = 6), or no immunosuppression [TAC(−)CPA(−)] (n = 6). In the TAC(+)CPA(−) and TAC(+)CPA(+) groups, tacrolimus (Prograf; Astellas, Japan) was

injected intramuscularly into the recipient rats at a dose of 0.64 mg/kg before and every day after transplantation. In TAC (+)CPA(+), candidate recipient rats were prepared with an intraperitoneal injection of cyclophosphamide (Endoxan, Shionogi, Japan) at a dose of 60 mg/kg 10 days before transplantation (dose of cyclophosphamide modified from previous report[18]). For Nagase analbuminemia rat recipients (n = 8), tacrolimus was given every day intramuscularly at a dose of 0.32 mg/kg. The recipient rats were observed daily and those in very poor condition were euthanized.

Evaluation of Luminescence From CLs

In vivo luciferase imaging of CLs was performed in both uPA/SCID mice for 3 months after hepatocyte transplantation and recipient rats throughout their survival after chimeric liver transplantation using a noninvasive bioimaging system (IVIS, Xenogen, CA), and the images were analyzed using a software package (Igor; Wave-Metrics, OR, and IVIS Living Image; Xenogen). Before imaging, D-luciferin (potassium salt; Biosynth, Switzerland) (30 mg/kg) was injected into the peritoneal cavity of uPA/SCID mice or the penile vein of recipient rats. Signal intensity was quantified as photon flux in units of photons (s/cm^2/steradian) in the region of interest.

ELISA for Serum Rat Albumin Levels

Blood samples were obtained from uPA/SCID mice for 3 months after hepatocyte transplantation and Nagase analbuminemia rat recipients for 4 months after chimeric liver transplantation. To examine hepatic functions specific to CLs in our model with an intact recipient liver, we measured serum rat albumin using a Rat Albumin ELISA KIT (AKRAL-120, Shibayagi, Japan).

Histological Analyses

Tissue samples were fixed in 10% formalin for hematoxylin-eosin staining, and 10-μm thick sections were used. For X-gal and immunohistochemical staining, 4%-paraformaldehyde-fixed frozen samples were sliced into 4-μm thick sections. X-gal analyses were performed as previously reported.[14] Immunohistochemical analyses of the CL grafts were performed before and 2 days after the host left lobectomy with anti-Ki67 rabbit polyclonal antibody (RB-1510-P, Thermo Fisher Scientific, CA). Fifteen random views of each sample were obtained and Ki67-positive hepatocytes were separately counted in areas (mm^2) with viable hepatocytes using image software (Scion Image; Scion, MD).

- 124 -

Ultrasonographic Analyses

Blood flow velocities were measured using an ultrasound system (Prosound SSD-α5; ALOKA, Japan). Velocity was quantified in unit of cm/second.

Statistical Analyses

We performed statistical analyses using StatView5.0 (SAS, NC). We used the analysis of variance test and Holm-Sidak as a post hoc test. Data are presented as the mean ± SEM, with values of $P < 0.05$ considered to be statistically significant.

RESULTS

Development of CL Grafts in Mice

On the basis of the repopulation of transplanted rat hepatocytes in uPA/SCID mice, the spreading of positive areas was observed using in vivo bioluminescent imaging (Fig. 2A). Luminescent fluxes increased rapidly and reached a plateau for approximately 3 months after hepatocyte transplantation (Fig. 2B). Moreover, serum rat albumin concentration on day 30 was significantly higher than that on day 5, then remained until day 85 (Fig. 2C). Luminescent fluxes and albumin concentrations were strongly correlated (Spearman correlation coefficient $r = 0.86$, $P < 0.0001$), suggesting that luminescence reflected CL function. The appearance was that of a normal mouse liver (Fig. 2D). Although hematoxylin-eosin staining showed normal histological structures, X-gal staining revealed that the mouse hepatic parenchyma was nearly entirely replaced by LacZ-positive rat hepatocytes, except for the other hepatic components, such as the vessels and bile ducts in Glisson capsules (Fig. 2E).

Graft Viability After Auxiliary Transplantation

In the TAC(−)CPA(−) group, luminescence vanished rapidly until day 5 after Chimeric liver transplantation, whereas it was stably maintained for 4 weeks in both TAC(+)CPA(−) and TAC(+)CPA (+). There was no significant difference between those 2 groups (Fig. 3A).

## Histological Analyses of Transplanted CL Grafts

Hematoxylin-eosin staining showed massive necrosis and destruction of the arrangement of the hepatic lobules in TAC(−)CPA(−) on day 5 (Fig. 3B). In contrast, TAC(+)CPA(−) on day 7 showed maintenance of those, even with massive cellular infiltration from the Glisson capsules to the central areas (Fig. 3C). Furthermore, in TAC(+)CPA(+), the hepatic structures were maintained with fewer rejection changes (Fig. 3D). Even on day 14, the TAC(+)CPA(+) protocol protected the CL from severe xenobiotic rejection, with only moderate cellular infiltration in the Glisson capsules (Fig. 3E).

Long-Term Patency of Reconstructed Vessel Circulations

Doppler ultrasonography showed the flow patterns of the arterial inflow and venous outflow in the transplanted CLs on days 14 and 188 in the TAC(+)CPA(−) group. Peak velocities on day 14 were 34.2 (artery) and 9.9 (vein) cm/s, whereas those on day 188 were 12.5 and 3.4 cm/s, respectively (See Figure, Supplemental Digital Content 3, available at http://links.lww.com/SLA/A257).

Long-Term Maintenance of Secretion of Rat Albumin in Nagase Analbuminemia Rats

Although serum rat albumin concentrations in Nagase analbuminemia rat recipients were undetectable before Chimeric liver transplantation, the transplanted CLs produced albumin on day 5 and then maintained production for 4 months, with maintenance of luminescence under the TAC(+)CPA(−) protocol (Fig. 4A).
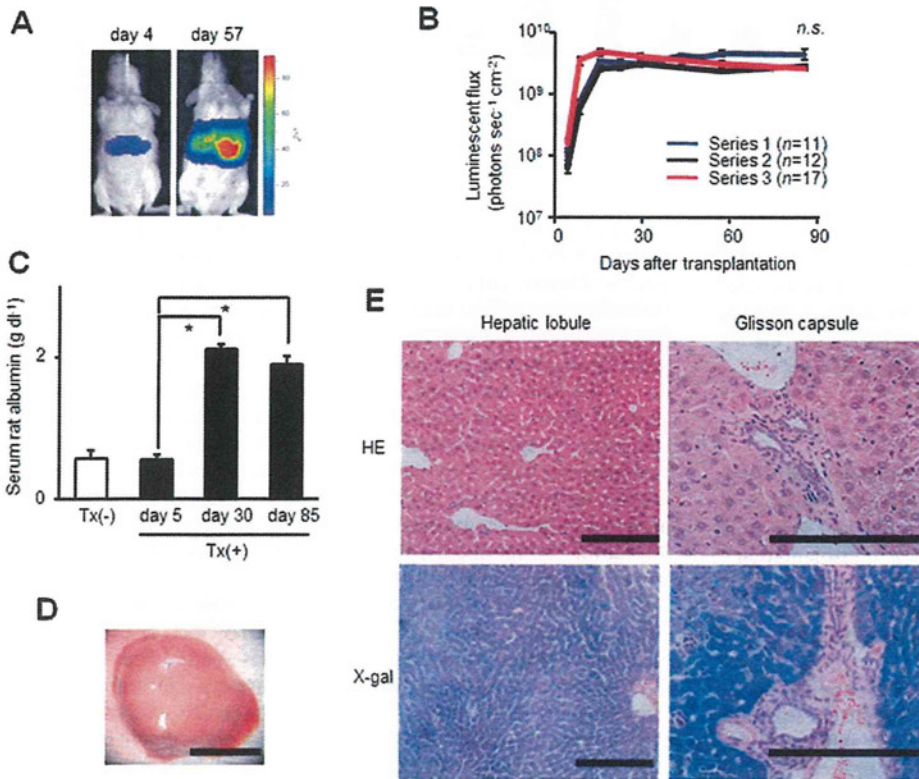
FIGURE 2. Development of CL grafts in uPA/SCID mice. A, Spread of luminescence-positive area. B, Luminescence after hepatocyte transplantation in 3 independent series. *n* as indicated; values are shown as the mean ± SEM; *n.s.*, no significant difference on day 85. C, Production of rat albumin by transplanted rat hepatocytes in mice ($n = 12$). *$P < 0.01$; Values are shown as the mean ± SEM; Tx, hepatocyte transplantation. D, Macroscopic appearance of CL before engraftment. Scale bar = 10 mm. E, hematoxylin-eosin and X-gal staining of intact CLs. The results shown are representative of 5 separate analyses. Scale bars = 200 μm.

- 125 -

FIGURE 3. Viability of transplanted CL grafts in wild-type LEW rat recipients. A, Luminescence from transplanted CLs. Each in vivo luminescent image is representative of 3 independent groups. *n* as indicated. B–E, Histological analyses of transplanted CLs. The figures present independent recipients. B, Graft with TAC(−)CPA(−) on day 5. C, Graft with TAC(+)CPA(−) on day 7. D, Graft with TAC(+)CPA(+) on day 4. E, Graft with TAC(+)CPA(+) on day 14. Scale bars = 200 μm.
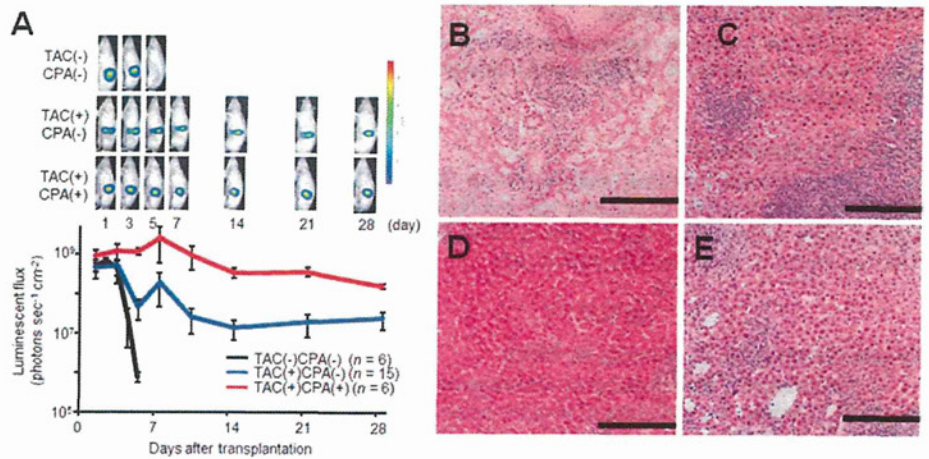
FIGURE 4. A, Luminescence (line) and albumin production (column) from transplanted CLs in Nagase analbuminemia rat recipients ($n = 3$). Values are shown as the mean ± SEM; pre, pre-chimeric liver transplantation. B–F, Immunohistochemical analyses with Ki67. B, C, Recipient native and transplanted CLs, respectively, before host hepatectomy. D, E, Recipient remnant and CLs, respectively, 2 days after recipient left lobectomy. F, Numbers of Ki67-positive cells. Values are shown as the mean ± SEM; pre, prelobectomy; post, postlobectomy.
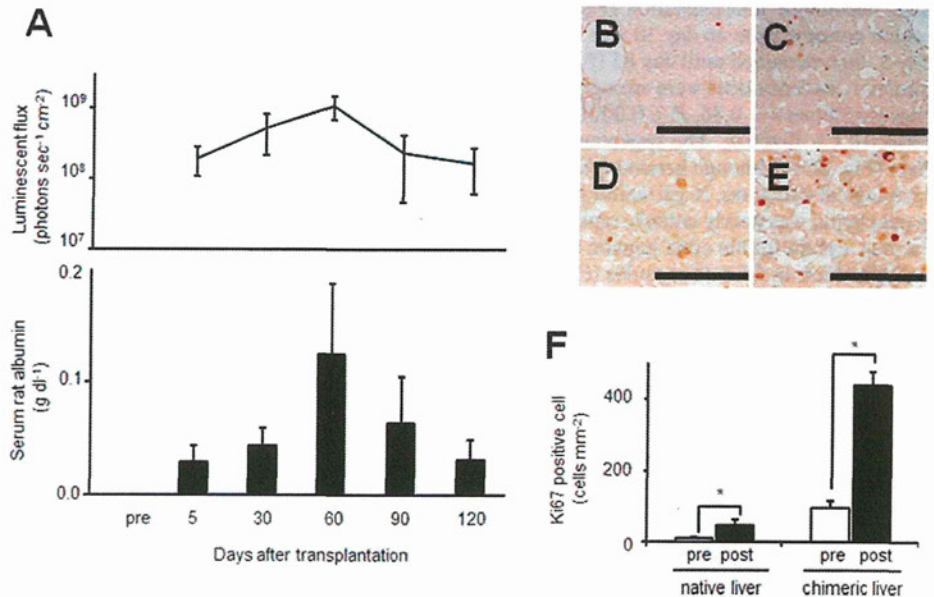
Self-Regenerative Capacity of Transplanted CL

Ki67 immunohistochemical analyses revealed that Ki67-positive cells were significantly increased in the CLs and in the remnant native livers at 2 days after the left lobectomy in the recipients, as compared with those sampled before the hepatectomy (Fig. 4B–F), suggesting the proliferative potential of the transplanted CLs.

DISCUSSION

The chronic shortage of liver grafts has led to extended criteria for grafts from both deceased[19,20] and living donors,[21] along with ethical issues related to organ trafficking and transplant tourism.[22] Although alternative therapies, such as hepatocyte transplantation,[23] transplantation from non–heart beating donors,[24] bioartificial liver,[25] and xenotransplantation,[26,27] have been intensively investigated to address this situation, none has been found practical because of low stability, low availability, and high antigenicity.

Regenerative approaches have recently been applied to develop engineered organs by focusing on native organs as scaffolds. An approach using a decellularized organ matrix enabled regeneration of syngeneic cells in an animal model,[5,6] though cell repopu-

lation efficiency was still low in ex vivo conditions. Another study injected blastocysts with xenogeneic pluripotent stem cells to produce a chimeric pancreas in a rodent model.[7] However, ubiquitous chimerism in scaffold animals has led to ethical concerns about the formation of chimeric brains and genitalia. Thus, effective and organ-specific engineering is required.

We have developed a strategy to create engineered chimeric "organ" livers with autologous or allogeneic human hepatocytes and other nonparenchymal components from xenogeneic scaffolds in transgenic pigs. This method enables utilization of patent hepatocytes and allogeneic donor cells, and the organogenetic potential in living animals contributes to rapid and timely production of CLs. Moreover, pretreatment with drugs or gene induction in the donor animal may be useful before transplantation.

In this study, we successfully created a rodent model to generate organ-specific engineered CLs, followed by their transplantation. CLs were created in uPA/SCID mice, whose native hepatocytes are injured through accumulation of urokinase-type plasminogen and provide a favorable niche for effective repopulation of transplanted hepatocytes from rats[28] and humans,[11] with a replacement rate greater than 90%.[12] Using hepatocytes derived from transgenic rats with

luciferase or LacZ genes, we found that transplanted hepatocytes in mice spread promptly and stably maintained their viability. Rat albumin production and histological analyses also indicated stable functions and structures of the CLs. These results demonstrated the advantages of CLs with effective productivity and maintenance. Because the CLs were one-eighth smaller than the rat native livers, we transplanted in an auxiliary manner without a hepatectomy or removal of the recipient liver. In addition, we removed the recipient's left kidney to utilize the left renal artery and vein as afferent and efferent vessels, respectively. We considered that a left nephrectomy would not have a large impact on our aim to investigate chimeric liver transplantation feasibility, whereas it might have an influence on recipient's survival. Moreover, though clinical liver transplantation and most rat liver transplantation models reconstruct portal vein circulation, we left it unanastomosed, as we previously reported in a rat auxiliary liver transplantation model,[17] in which the transplanted livers maintained their histological structure.

This analysis revealed severe rejection toward xenogeneic components, resulting in disappearance of luminescence in CLs without immunosuppression. Because humoral rejection was suspected in xenorejection toward the vascular endothelium,[29] we used cyclophosphamide to suppress antibody production in addition to tacrolimus.[18] Our results showed improvement in graft survival in the immunosuppressed groups. TAC(+)CPA(+) showed higher luminescence as compared with TAC(+)CPA(−), though there was no statistical difference between them. On the other hand, histological results showed the superiority of TAC(+)CPA(+). We speculated that these findings indicated antibody-mediated rejection even in Chimeric liver transplantation and that appropriate combination therapies might improve graft survival. Although we previously hypothesized that syngeneic parenchyma might function to protect against rejection toward xeno-components,[30] the reaction to mouse-origin tissues remained without obvious evidence of attenuation. Further studies to investigate the effects of hepatocytes and specific targets of rejection are required, including those that focus on other aspects such as genetic expressions.[31]

In clinical liver transplantation, thrombotic events can result in graft failure.[32] Ultrasonography showed arterial and venous flow in transplanted CLs even after 6 months, which indicated patency of the anastomosed vessels. We also investigated rat albumin in Nagase analbuminemia rat recipients and demonstrated stable production for a long period. Although the liver possesses a variety of functions and markers,[3,6] albumin analysis showed functions specific to transplanted CLs in Nagase analbuminemia rats with intact livers, which functioned normally except for albumin production. We regarded this result to be preferable in regard to our aim to investigate the feasibility of Chimeric liver transplantation to show those functions in vivo. Interestingly, we found stable luminescence in transplanted CLs of Nagase analbuminemia rat recipients whose hepatocytes were allogeneic to those of other recipients (RT1[l] vs RT1[a]), suggesting the possibility of a hepatocyte bank for use in producing CLs in clinical settings.

Ki67 analyses showed that hepatocytes in the transplanted CLs maintained proliferation potential. Patients with end-stage liver disease are thought to manifest increasing serum hepatotropic growth signals, such as hepatocyte growth factor.[33] It is expected that CLs will have the potential to respond to such signals to maintain and improve viability after transplantation.

Judging from recent technological achievements in transgenic animals, and ethical issues related to primate usage and practical issues of availability and body size, transgenic pigs represent a major candidate for scaffold animals. Although transgenic pigs such as alpha-1,3-galactosyltransferase gene knockout and human decay accelerating factor transgenic pigs show reduced immunological re-

sponses toward the host, complete rejection suppression remains difficult and development of appropriate immunosuppressive protocols is important. Moreover, replacement of nonhepatocyte components, especially vascular endothelium, in the CLs of scaffold pigs or development of humanized pigs is expected. However, utilization of xenogeneic porcine scaffolds raise concerns about xenozoonosis such as porcine endogenous retrovirus,[34,35] though the practical possibility of transmission remains uncertain and some reports have shown results without obvious infection.[36] Nevertheless, cautious and longer investigations are indispensable to secure patient safety.

Although further studies that compare conventional liver transplantation models with this model and larger animal models are needed, the realization of this bioengineering strategy with cell sources and transgenic animals might ultimately lead to replacement of human grafts and achievement of liver transplantation without human donors. These results should provide an important contribution toward scaffold-focused engineering of livers and engineered organ transplantation.

CONCLUSIONS

Engineered CLs were successfully transplanted and showed maintenance of function and structure for a long period. Our results suggest that such CLs have potential to be utilized as alternative grafts.

ACKNOWLEDGMENTS

REFERENCES

1. Thuluvath PJ, Guidinger MK, Fung JJ, et al. Liver transplantation in the United States, 1999–2008. *Am J Transplant.* 2010;10:1003–1019.

2. Yeh H, Smoot E, Schoenfeld DA, et al. Geographic inequity in access to livers for transplantation. *Transplantation.* 2011;91:479–486.

3. Ohashi K, Yokoyama T, Yamato M, et al. Engineering functional two- and three-dimensional liver systems in vivo using hepatic tissue sheets. *Nat Med.* 2007;13:880–885.

4. Soto-Gutiérrez A, Kobayashi N, Rivas-Carrillo JD, et al. Reversal of mouse hepatic failure using an implanted liver-assist device containing ES cell-derived hepatocytes. *Nat Biotechnol.* 2006;24:1412–1419.

5. Ott HC, Matthiesen TS, Goh SK, et al. Perfusion-decellularized matrix: using nature's platform to engineer a bioartificial heart. *Nat Med.* 2008;14:213–221.

6. Uygaun BE, Soto-Gutierrez A, Yagi H, et al. Organ reengineering through development of a transplantable recellularized liver graft using decellularized liver matrix. *Nat Med.* 2010;16:814–820.

7. Kobayashi T, Yamaguchi T, Hamanaka S, et al. Generation of rat pancreas in mouse by interspecific blastocyst injection of pluripotent stem cells. *Cell.* 2010;142:787–799.

8. Ekser B, Rigotti P, Gridelli B, et al. Xenotransplantation of solid organs in the pig-to-primate model. *Transpl Immunol.* 2009;21:87–92.

9. Klymiuk N, Aigner B, Brem G, et al. Genetic modification of pigs as organ donors for xenotransplantation. *Mol Reprod Dev.* 2010;77:209–221.

10. Locke JE, Sun Z, Warren DS, et al. Generation of humanized animal livers using embryoid body-derived stem cell transplant. *Ann Surg.* 2008;248:487–493.

11. Mercer DF, Schiller DE, Elliott JF, et al. Hepatitis C virus replication in mice with chimeric human livers. *Nat Med.* 2001;7:927–933.

12. Tateno C, Yoshizane Y, Saito N, et al. Near completely humanized liver in mice shows human-type metabolic responses to drugs. *Am J Pathol.* 2004;165:901–912.

13. Hakamata Y, Murakami T, Kobayashi E. "Firefly rats" as an organ/cellular source for long-term in vivo bioluminescent imaging. *Transplantation.* 2006;81:1179–1184.

14. Horie M, Sekiya I, Muneta T, et al. Intra-articular injected synovial stem cells differentiate into meniscal cells directly and promote meniscal regeneration without mobilization to distant organs in rat massive meniscal defect. *Stem Cells.* 2009;27:878–887.

15. Oren R, Dabeva MD, Petkov PM, et al. Restoration of serum albumin levels in Nagase analbuminemic rats by hepatocyte transplantation. *Hepatology.* 1999;29:75–81.

16. Enosawa S, Suzuki S, Li XK, et al. Higher efficiency of retrovirus transduction in the late stage of primary culture of hepatocytes from nontreated than from partially hepatectomized rat. *Cell Transplant.* 1998;7:413–416.

17. Rong Xiu D, Hishikawa S, Sato M, et al. Rat auxiliary liver transplantation without portal vein reconstruction: comparison with the portal vein-arterialized model. *Microsurgery.* 2001;21:189–195.

18. Murase N, Starzl TE, Demetris AJ, et al. Hamster-to-rat heart and liver xenotransplantation with FK506 plus antiproliferative drugs. *Transplantation.* 1993;55:701–708.

19. Durand F, Renz JF, Alkofer B, et al. Report of the Paris consensus meeting on expanded criteria donors in liver transplantation. *Liver Transpl.* 2008;14:1694–1707.

20. Renz JF, Kin C, Kinkhabwala M, et al. Utilization of extended donor criteria liver allografts maximizes donor use and patient access to liver transplantation. *Ann Surg.* 2005;242:556–565.

21. Trotter JF, Adam R, Lo CM, et al. Documented deaths of hepatic lobe donors for living donor liver transplantation. *Liver Transpl.* 2006;12:1485–1488.

22. Steering Committee of the Istanbul Summit. Organ trafficking and transplant tourism and commercialism: the Declaration of Istanbul. *Lancet.* 2008;372:5–6.

23. Dhawan A, Puppi J, Hughes RD, et al. Human hepatocyte transplantation: current experience and future challenges. *Nat Rev Gastroenterol Hepatol.* 2010;7:288–298.

24. Selck FW, Grossman EB, Ratner LE, et al. Utilization, outcomes, and retransplantation of liver allografts from donation after cardiac death: implications for further expansion of the deceased-donor pool. *Ann Surg.* 2008;248:599–607.

25. Demetriou AA, Brown RS, Busuttil RW, et al. Prospective, randomized, multicenter, controlled trial of a bioartificial liver in treating acute liver failure. *Ann Surg.* 2004;239:660–670.

26. Starzl TE, Fung J, Tzakis A, et al. Baboon-to-human liver transplantation. *Lancet.* 1993;341:65–71.

27. Ekser B, Gridelli B, Tector AJ, et al. Pig liver xenotransplantation as a bridge to allotransplantation: which patients might benefit? *Transplantation.* 2009;88:1041–1049.

28. Giannini C, Morosan S, Tralhao JG, et al. A highly efficient, stable, and rapid approach for ex vivo human liver gene therapy via a FLAP lentiviral vector. *Hepatology.* 2003;38:114–122.

29. Ghebremariam YT, Smith SA, Anderson JB, et al. Intervention strategies and agents mediating the prevention of xenorejection. *Ann N Y Acad Sci.* 2005;1056:123–143.

30. Goto S, Lord R, Kobayashi E, et al. Novel immunosuppressive proteins purified from the serum of liver-retransplanted rats. *Transplantation.* 1996;61:1147–1151.

31. Tahara K, Murakami T, Fujishiro J, et al. Regeneration of the rat neonatal intestine in transplantation. *Ann Surg.* 2005;242:124–132

32. Bekker J, Ploem S, de Jong KP. Early hepatic artery thrombosis after liver transplantation: a systematic review of the incidence, outcome and risk factors. *Am J Transplant.* 2009;9:746–757.

33. Tomiya T, Omata M, Imamura H, et al. Impaired liver regeneration in acute liver failure: the significance of cross-communication of growth associated factors in liver regeneration. *Hepatol Res.* 2008;38:S29–S33.

34. Mueller NJ, Takeuchi Y, Mattiuzzo G, at al. Microbial safety in xenotransplantation. *Curr Opin Organ Transplant.* 2011;16:201–206.

35. Onions D, Cooper DK, Alexander TJ, et al. An approach to the control of disease transmission in pig-to-human xenotransplantation. *Xenotransplantation.* 2000;7:143–155.

36. Michaels MG, Kaufman C, Volberding PA, et al. Baboon bone-marrow xenotransplant in a patient with advanced HIV disease: case report and 8-year follow-up. *Transplantation.* 2004;78:1582–1589.

- 128 -

BRIEF ARTICLE

A novel animal model for *in vivo* study of liver cancer metastasis

Shinsuke Fujiwara, Hikaru Fujioka, Chise Tateno, Ken Taniguchi, Masahiro Ito, Hiroshi Ohishi, Rie Utoh, Hiromi Ishibashi, Takashi Kanematsu, Katsutoshi Yoshizato

Shinsuke Fujiwara, Hikaru Fujioka, Ken Taniguchi, Masahiro Ito, Hiromi Ishibashi, Clinical Research Center, National Hospital Organization Nagasaki Medical Center and Division of Hepatology, Nagasaki University Graduate School of Biomedical Sciences, Nagasaki 856-8652, Japan
Chise Tateno, Hiroshi Ohishi, Katsutoshi Yoshizato, Liver Research Laboratory, PhoenixBio Co., Ltd, Hiroshima 739-8511, Japan
Chise Tateno, Rie Utoh, Katsutoshi Yoshizato, Yoshizato Project, CLUSTER, Hiroshima Prefectural Institute of Industrial Science and Technology, Hiroshima 739-8511, Japan
Takashi Kanematsu, Division of Surgery II, Nagasaki University Graduate School of Biomedical Sciences, Nagasaki 856-8652, Japan
Katsutoshi Yoshizato, Liver Research Center, Osaka City University, Graduate School of Medicine, Osaka 532-0025, Japan
Author contributions: Fujiwara S, Fujioka H and Taniguchi K designed research; Tateno C, Ohishi H, and Utoh R contributed new agents/analytic tools; Fujiwara S, Fujioka H, Ito M, Ishibashi H and Kanematsu T analyzed data; and Fujiwara S, Fujioka H and Yoshizato K wrote the paper.
Supported by CLUSTER-Yoshizato Project and the National Hospital Organization Nagasaki Medical Center
Correspondence to: Shinsuke Fujiwara, MD, Clinical Research Center, National Hospital Organization Nagasaki Medical Center and Division of Hepatology, Nagasaki University Graduate School of Biomedical Sciences, 2-1001-1 Kubara, Omura, Nagasaki 856-8652, Japan. gearorange@nmc-research.jp
Telephone: +81-957-523121 Fax: +81-957-536675
Received: November 25, 2011 Revised: January 25, 2012
Accepted: April 21, 2012
Published online: August 7, 2012

Abstract

AIM: To establish an animal model with human hepatocyte-repopulated liver for the study of liver cancer metastasis.

METHODS: Cell transplantation into mouse livers was conducted using alpha-fetoprotein (AFP)-producing human gastric cancer cells (h-GCCs) and h-hepatocytes as donor cells in a transgenic mouse line expressing urokinase-type plasminogen activator (uPA) driven by the albumin enhancer/promoter crossed with a severe combined immunodeficient (SCID) mouse line (uPA/SCID mice). Host mice were divided into two groups (A and B). Group A mice were transplanted with h-GCCs alone, and group B mice were transplanted with h-GCCs and h-hepatocytes together. The replacement index (RI), which is the ratio of transplanted h-GCCs and h-hepatocytes that occupy the examined area of a histological section, was estimated by measuring h-AFP and h-albumin concentrations in sera, respectively, as well as by immunohistochemical analyses of h-AFP and human cytokeratin 18 in histological sections.

RESULTS: The h-GCCs successfully engrafted, repopulated, and colonized the livers of mice in group A (RI = 22.0% ± 2.6%). These mice had moderately differentiated adenocarcinomatous lesions with disrupted glandular structures, which is a characteristics feature of gastric cancers. The serum h-AFP level reached 211.0 ± 142.2 g/mL (range, 7.1-324.2 g/mL). In group B mice, the h-GCCs and h-hepatocytes independently engrafted, repopulated the host liver, and developed colonies (RI = 12.0% ± 6.8% and 66.0% ± 12.3%, respectively). h-GCC colonies also showed typical adenocarcinomatous glandular structures around the h-hepatocyte-colonies. These mice survived for the full 56 day-study and did not exhibit any metastasis of h-GCCs in the extrahepatic regions during the observational period. The mice with an h-hepatocyte-repopulated liver possessed metastasized h-GCCs and therefore could be a useful humanized liver animal model for studying liver cancer metastasis *in vivo*.

CONCLUSION: A novel animal model of human liver cancer metastasis was established using the uPA/SCID mouse line. This model could be useful for *in vivo* testing of anti-cancer drugs and for studying the mechanisms of human liver cancer metastasis.

Peer reviewer: Samir Ahboucha, Équipe NPE, Cadi Ayyad University, Avenue My Abdellah, Marrakesh 40000, Morocco

INTRODUCTION

Tumor metastasis, which is defined by a process in which tumor cells originating from an organ invade another anatomically distant organ, is the leading cause of cancer-related mortality[1,2]. One of the major target organs for cancer metastasis is the liver[1-3], and therefore there is increasing need for animal models that accurately mimic the pathophysiological situations in human liver and are suitable for investigating the mechanisms of hepatic cancer metastasis. In fact, several studies have attempted to transplant metastatic h-tumor cells into the livers of the immuno-compromized mice, such as athymic nude mice[4], which cannot generate T cells, severe combined immunodeficient (SCID) mice that lack mature B and T cells[5-7], and NOD/SCID/c^{null} (NOG) mice[8,9], which are deficient in T, B, and natural killer cells, and have impaired dendritic cells. In these animal models, the transplanted h-tumor cells invade the hepatic parenchyma, which is composed of mouse hepatocytes that are phylogenetically distant from h-hepatocytes and are known to exhibit biological and pathological features that are different from the human counterpart.

Heckel *et al*[10] established transgenic mice expressing urokinase type plasminogen activator (uPA) under the control of the albumin (Alb) enhancer/promoter and found that the m-hepatocytes were constitutively damaged due to constant exposure to the expressed uPA. In another study, a mouse line possessing a humanized liver (chimeric mouse) was generated by transplanting healthy and normal h-hepatocytes into the liver of the immuno- and liver-compromized mouse, which was created by mating the uPA-Tg mouse with the SCID mouse (uPA/SCID mouse)[10,11].

We previously developed chimeric mice where the liver was stably and reproducibly replaced with h-hepatocytes and found that the occupancy ratio or replacement index (RI) in the parenchyma was quite high (> 90%) in best cases[12]. Human hepatocytes in the chimeric m-liver have been intensively and extensively characterized based on normal hepatic phenotypes, such as expres-

sion profiles of cytochrome P450, the major xenobiotic-metabolizing enzymes, drug-metabolizing capacities, and hepatitis virus infectivity[11,13-15]. Based on these studies, which indicate that a chimeric m-liver can appropriately recapitulate the characteristics of h-liver, we hypothesized that the chimeric mouse as an animal model can be used to investigate the underlying mechanisms of tumor metastasis into the liver where the parenchyma is largely composed of normal and healthy h-hepatocytes.

In the present study, we established a chimeric mouse as a novel experimental model that sufficiently mimics the pathophysiological micro-environment in h-liver for studying liver cancer metastasis.

MATERIALS AND METHODS

This study was approved by the Ethics Committee of the National Hospital Organization, Nagasaki Medical Center, the Hiroshima Prefectural Institute of Industrial Science and Technology Ethics Board, and the Phoenix-Bio Ethics Board. This study was conducted in accordance with their guidelines.

Animals

The uPA/SCID mice were generated and used as transplant hosts once they reached an age of 24-32 d old as previously described[14,15]. The mice were maintained in the laboratory in a specific pathogen-free environment in accordance with the guidelines of the Hiroshima Prefectural Institute of Industrial Science and Technology Ethics Board as well as the PhoenixBio Ethics Board.

Cancer cells

Human gastric cancer cells (h-GCCs) were purchased from the Japanese Collection of Research Biosources (Osaka, Japan) and used as liver metastatic cancer cells. These cells are adenocarcinoma cells derived from human gastric cancer cells that produce alpha-fetoprotein (AFP) and have a high affinity for liver tissue[16-18]. The cells were maintained in Dulbecco's modified Eagle's medium (Sigma Chemical Co., St. Louis, MO, United States) containing 10% fetal bovine serum (Sigma Chemical Co., St. Louis, MO, United States) in an atmosphere of 95% air and 5% CO_2 at 37 ℃.

Cell transplantation into the uPA/SCID

Human GCCs were suspended at a concentration of 1 × 10^7 cells/mL and placed on ice until transplantation. Cryopreserved h-hepatocytes derived from a 6-year-old African female were purchased from BD Biosciences (San Jose, CA, United States), thawed in a 37 ℃ water bath, rapidly diluted with culture medium at 4 ℃, and washed twice to remove the cryopreservation solution. The cell viability was assessed by a trypan blue exclusion test. The uPA/SCID mice were anesthetized with ether and then were intrasplenically injected with the h-hepatocytes as previously described[12]. Blood samples, 5 μL each, were periodically collected from the host tail-vein for

Table 1 Serum concentrations of human albumin and human alpha-fetoprotein in host mice at 56 d post-transplantation

Experimental groups	Transplanted cells	No. of animals	Serum concentration	
			h-Alb (mg/mL)	h-AFP (mg/mL)
A	h-GCCs	4	UD	7.1-324.2
				(211.0 ± 142.2)
B	h-GCCs and h-hepatocytes	6	0.03-9.1 (3.1 ± 3.5)	0.3-126.1 (54.3 ± 60.7)

The numerals represent the range of the concentrations and those in the parentheses indicate the mean ± SD. h-GCCs: Human gastric cancer cells; h-Alb: Human albumin; h-AFP: Human alpha-fetoprotein; h-hepatocytes: Human hepatocytes; UD: Undetectable.

determining concentrations of human albumin (h-Alb) and human AFP (h-AFP) using an h-Alb enzyme-linked immunosorbent assay quantification kit (Bethyl Laboratories Inc., Montgomery, TX) and an h-AFP enzyme immunoassay test kit (Hope Laboratories, Belmont, CA, United States), respectively.

Histological and immunohistochemical evaluation of the m-liver

Liver tissue specimens were removed from the transplanted mice, paraffin-embedded, sectioned at a 4 μm thickness, and stained with hematoxylin and eosin (H and E). Human hepatocyte-colonies were identified by staining the sections with mouse monoclonal antibodies against human-specific cytokeratin 18 (h-CK18) (DAKO, Glostrup Denmark). Human GCCs in the m-liver were identified by h-AFP staining with a polyclonal Ab (Novocastra Laboratories Ltd, United Kingdom). The sections were treated with a biotinylated, goat anti-rabbit IgG for h-CK18 and rabbit anti-m-IgG (DAKO, Glostrup Denmark) for h-AFP. All of the tissue specimens or cells were counterstained with H and E.

Determination of h-hepatocytes and h-GCCs repopulation of the uPA/SCID m-liver

Serial liver sections were double immunostained for h-CK18 and h-AFP to identify h-hepatocytes/h-GCCs and h-GCCs, respectively. The extent of repopulation of h-hepatocytes and h-GCCs in the chimeric mouse liver was determined as the RI, which is the occupational ratio of the transplanted cells in the examined area of histological sections, as previously described[12]. The RI of h-hepatocytes (RIh-hepatocytes) in the uPA/SCID m- liver was determined using h-CK18 as a maker to histologically identify h-hepatocytes. When appropriate, the RI for h-GCCs (RIh-GCCs) was referred to as the metastatic index (MIh-GCCs) in this study. Human hepatocytes and h-GCCs were identified on histological sections as the h-CK18-positive (h-CK18+) and h-AFP-negative (h-AFP-) cells and the h-CK18+ and h-AFP+ cells, respectively. The RIh-hepatocytes and MIh-GCC of the m- livers were calculated as the ratio of the "h-CK18+/h-AFP-" and "h-CK18+/h-AFP+" areas to the entire examined area of the sections, respectively.

Experimental groups

The uPA/SCID mice were divided into two groups (A and B groups). Four uPA/SCID mice in group A were each injected with 1×10^6 h-GCCs. Six mice in group B were co-transplanted with 7.5×10^5 h-hepatocytes and h-GCCs each. The blood h-Alb and h-AFP concentrations were periodically monitored after cell transplantation. The mice were euthanized at the termination of the experiments and their livers, spleens, and lungs were microscopically examined to identify any metastasis of h-GCCs.

RESULTS

Group A experiment

Human GCCs were transplanted into the livers of uPA/SCID mice and euthanized 56 d after transplantation. Human GCC colonies were macroscopically distinguishable from the host m-liver cells as brown colored regions (Figure 1A). Histological examinations showed that these areas contained h-GCC colonies and host m-liver cells composed of m-parenchymal and m-nonparenchymal cells (Figure 1B). The whitish or pale regions observed in Figure 1A were composed of only m-liver cells. The specimens were also stained for h-AFP to define h-GCCs (Figure 1C and D). Human GCCs formed colonies with well-developed glandular structures, which is a characteristic feature of gastric cancer. The serum concentrations of h-AFP increased to 211.0 ± 142.2 g/mL (range 7.1-324.2 g/mL, Table 1), which reflected the repopulation of h-GCCs in the liver, since serum h-AFP was undetectable in uPA/SCID mice without transplantation of h-GCCs (data; not shown). The MI of h-GCCs (MIh-GCC) was 22.0% ± 2.6% at the termination of the experiment 56 d post-transplantation.

Group B experiment

Both h-hepatocytes and h-GCCs were simultaneously transplanted into six uPA/SCID mice. The serum concentrations of h-Alb and h-AFP monitored after the cell transplantation (Figure 2). These protein levels were variable among individual mice, and three mice (No. 1-3) had substantially elevated h-Alb levels over the 56-d study. In addition, these mice exhibited RIh-hepatocytes > 70% based on the correlation graph between h-Alb concentrations and RISh-hepatocytes[12]. These hosts also had markedly elevated h-AFP concentrations. In particular, mice No. 1 and 2 showed the highest h-Alb levels (approximately 9.1 mg/mL) and h-AFP concentrations (approximately 126.1 mg/mL) at 56 d post-transplantation (Table 1; Figure 2). As shown in Figure 3A, mouse 1 had the highest h-Alb and h-AFP levels, and the liver was composed of brown and whitish regions indicated by the thick and the thin arrows, respectively, which corresponded to the colonies composed of both h-hepatocytes and h-GCCs or m-liver cells, respectively. The brown region in the liver shown in Figure 3A was sectioned and stained with H and E (Figure 3B), anti-h-CK18 Abs to identify both h-hepatocytes and
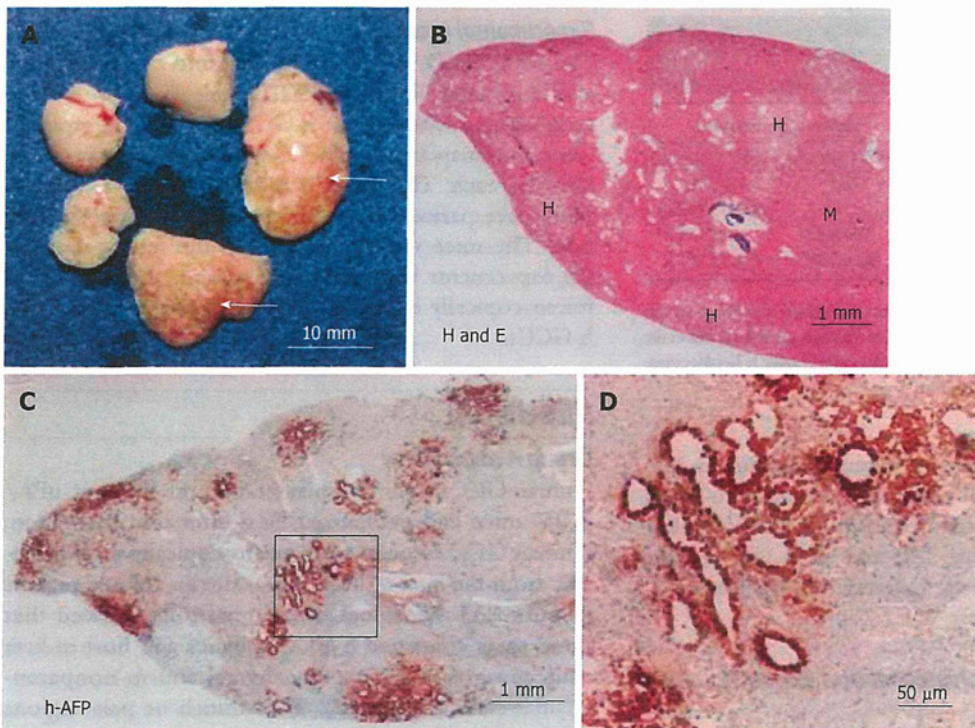
Figure 1 Macro- and microscopic images of the liver from group A mice. A: The urokinase-type plasminogen activator/severe combined immunodeficient mouse mice were transplanted with human gastric cancer cells (h-GCCs) and euthanized 56 d later, at which time the livers were isolated and photographed; B: The arrows in A point to concentrated regions of h-GCC colonies, and the sections were stained with hematoxylin and eosin (H and E). H and M in B represent h-GCC colonies and m-liver cell regions, respectively; C: The sections were stained with anti-human alpha-fetoprotein (h-AFP) antibodies; D: The square region in C is enlarged and shown.
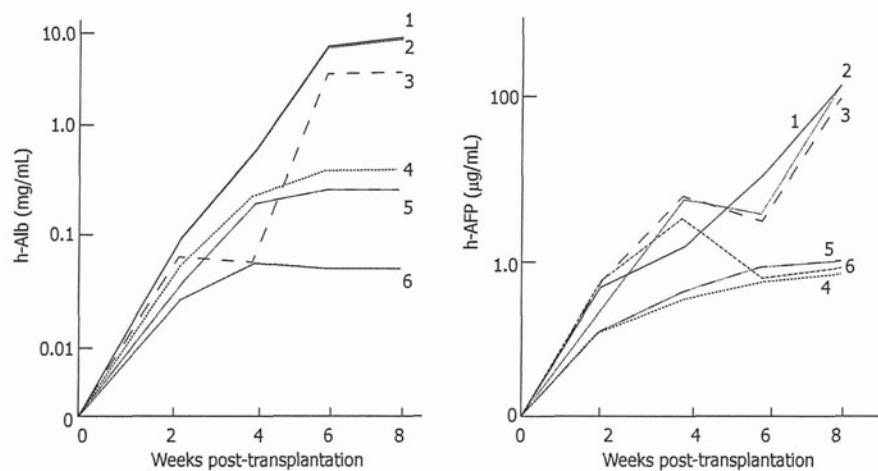
Figure 2 Changes in the serum concentrations of human albumin and human alpha-fetoprotein in group B-mice. Six mice (No.1-6) were co-transplanted with h-hepatocytes and human gastric cancer cells. The serum levels of human albumin (h-Alb) (left panel) and human alpha-fetoprotein (h-AFP) (right panel) were periodically monitored after the cell transplantation.

h-GCCs (Figure 3C), and the anti-h-AFP Ab to identify h-GCCs (Figure 3D). A comparison of Figure 3B and C showed that most of the section from Figure 3B was occupied with h-CK18$^+$ cells, which corresponded to the cells in the less eosinophilic areas of the H and E section. Human CK18$^-$ m-liver cells were located in eosinophilic areas in the H and E section, which were sporadically distributed as clusters with variable forms among large engrafted h-cell colonies. Human-AFP$^+$ h-GCC-colonies were distinguished by comparing Figure 3B-D. These colonies were surrounded with less eosinophilic

h-hepatocytes (Figure 3D) that were swollen and clearer (Figure 3B and C). Magnified views of the brown area obtained from another serial sections of the liver shown in Figure 3A are shown in Figure 4A (H and E) and Figure 4B (h-AFP-stain). Human GCCs formed moderately differentiated adenocarcinomas with disrupted glandular structures, which is a characteristic feature of gastric cancer. Morphometric analyses using these h-CK18- and h-AFP-stained serial sections indicated that the RI$_{h-hepatocyte}$ and MI$_{h-GCC}$ in group B mice was 66.0% ± 12.3% (n = 6) and 12.0% ± 6.8% (n = 6), respectively. The mice in
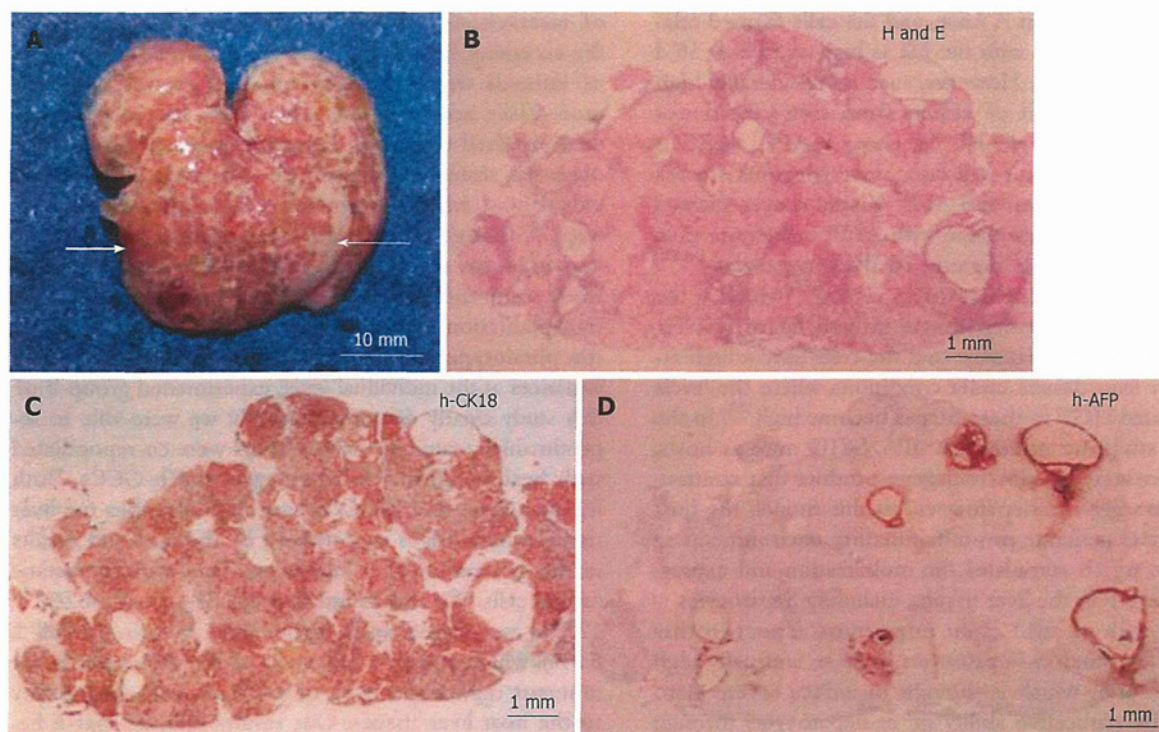
Figure 3 Macroscopic image of the liver of mouse No. 1 from Figure 2 at 56 d post-transplantation. A: The thick and thin white arrows point to h-cells [human hepatocytes (h-hepatocytes) and human gastric cancer cells (h-GCCs)] and m-liver cell regions, respectively; B: The liver was sectioned and stained with hematoxylin and eosin (H and E); C: The liver was sectioned and stained with anti-h-CK18; D: The liver was sectioned and stained with anti-human alpha-fetoprotein (h-AFP) antibodies. The h-AFP + (h-GCC) colonies were surrounded by less eosinophilic h-hepatocytes.
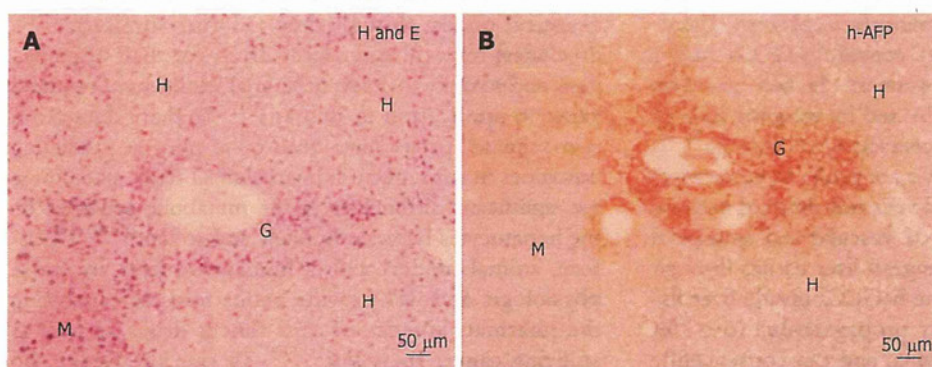
Figure 4 Magnified images of hepatic histology from group B mice. A: A serial section of the liver in Figure 3 was subjected to hematoxylin and eosin (H and E); B: A serial section of the liver in Figure 3 was subjected to human alpha-fetoprotein (h-AFP) staining. H, G and M represent the areas occupied by human-hepatocytes, human gastric cancer cells (h-GCCs), and host m-liver cells, respectively. h-GCCs composed moderately differentiated adenocarcinoma with disrupted glandular structures.

group B survived for the entire 56 d study. Extrahepatic sites and organs, such as the peritoneal cavity and kidney, were also examined for the presence of metastatic h-GCC lesions. The metastatic h-GCCs were not found in the extrahepatic regions during the observational period, indicating that the cells did not metastasize to any other regions.

DISCUSSION

An ideal animal model for liver metastasis of h-cancer cells should possess at least two key features. First, the transplanted cancer cells need to invade and colonize in the host liver. Second, the liver of the host model has to provide the human cells with appropriate pathophysiological microenvironments that recapitulate the h-liver *in vivo*. Most of the conventional models to date manifest the first feature, but none of them have been able to sufficiently recapitulate the microenvironment of the h-liver [4-6]. In the present study, we established a unique and novel that possessed both of these features.

In our study, we successfully engrafted the liver with

h-GCCs in the group A mice, and the cells formed relatively large colonies, with the MI as high as 25% at 56 d post-transplantation. However, such a considerably high MI could be a result of effects from either the donor or host side of the model. We chose h-AFP[+] h-GCCs as a metastatic cancer cell line, since previous studies reported that patients with AFP[+] gastric cancer showed a higher liver MI than those with AFP^{-} cells; more than 70% of the patients developed liver metastasis[18,19]. These AFP^{+} cancer cells express c-Met[19], which is the receptor for human hepatocyte growth factor (HGF), and therefore it is plausible that the cells have a high affinity for liver tissues under conditions where the levels of activated HGF in these tissues become high [20]. In the present study, we utilized the uPA/SCID mice as hosts, which possessed a uPA transgene product that continuously damages the hepatocytes. In this model, the host hepatocytes generate pro-inflammatory environments in the liver, which stimulates the mobilization and expression of HGF in the liver tissues, including hepatocytes.

The role of uPA is an important aspect in this model. The host m-hepatocytes express unusually high levels of uPA, which is thought to induce severe damage in the replicative ability of m-hepatocytes through the activation of plasminogen, fibrinogen, and other proteins within the rough endoplasmic reticulum (RER) involved in proteolysis that lead to functional defects of the RER[21]. In addition, uPA is secreted from m-hepatocytes into the plasma[10], indicating that it circulates to liver tissues through sinusoidal capillaries and activates the conversion of blood plasminogen to plasmin. Therefore, the host liver tissue may provide h-GCCs with a pro-metastatic-like microenvironment. In fact, previous studies have indicated that uPA and its receptor (uPAR) play critical roles in the extravasation of tumors[22-24]. Therefore, the injected h-GCCs are prone to extravasate liver tissues through the portal vein and sinusoid because of the uPA-induced fragility of vascular and sinusoidal endothelia and subsequently engraft liver tissues through an affinity for c-Met. Once the h-GCCs invade liver tissues, they can relatively easily propagate due to c-Met signaling in the host parenchyma, and can consequently replace m-hepatocytes as a result of the uPA-mediated damage. These conditions are also convenient for engraftment and proliferation of normal, healthy h-hepatocytes, as shown in this study when co-transplanted with h-GCCs.

The co-transplantation of h-hepatocytes with h-GCCs also resulted in the development of metastatic colonies in the mice similar to the transplantation of h-GCCs alone. In this type of transplantation experiment, large variances in serum concentrations of replacement marker proteins (h-Alb and h-AFP) were observed. The h-AFP kinetic curves were different from those of h-Alb and exhibited an increase of the serum level through "three steps": initial increase, followed by a plateau or decline, and then a sharp increase. This complex h-AFP kinetic pattern suggests the presence of interactions between the invading cancer cells and the accepting host cells. There seemed to be two groups of animals within the experimental groups, one that more easily accepted xenogeneic cells and another that demonstrated resistance. However, we have consistently observed similar variances in h-Alb levels among individual mice when we generated h-hepatocyte chimeric mice[12], though inbred mice were used as hosts. These variances are accidental in nature and might originate from some differences in manipulation procedures for transplantation as well as uncontrollable differences in the phenotypes of the uPA Tg mice[10]. Despite these variances at the individual level, experimental group B of this study clearly demonstrated that we were able to reproducibly create mice whose livers were co-repopulated with healthy, normal h-hepatocytes and h-GCCs. Both h-hepatocytes and h-GCCs have high affinities for liver tissue, which drives engraftment of the liver and results in the generation of a humanized liver with metastatic cancer cells. We also found that the RI$_{\text{h-hepatocyte}}$ (66.0% ± 12.3%) was significantly higher than MI$_{\text{h-GCC}}$ (12.0% ± 6.8%), which may be a reflection of the difference in the inherent replication rates of the cells and adaptability to the host liver tissues. Our results indicate that h-hepatocytes are, as a whole, superior to h-GCCs in colony growth.

Relevant and reproducible animal models are indispensable tools for deducing the mechanisms of liver metastasis and pharmacokinetics of anti-cancer drugs, and several models have been developed to meet these practical needs, though they are quite limited[2,25-30]. Preclinical tests of anti-cancer drugs for their effectiveness and toxicity in relevant animal models are required prior to application in humans[31]. Toxicity data from non-primate species have been quite poor at predicting outcomes in subsequent human clinical trials, since there are significant differences in the metabolic activities of the hepatocytes between humans and rodent[32-34]. Therefore, animal models with a humanized liver are more physiologic and will provide better tools for analyzing the pharmacokinetics of anti-cancer drugs as well as studying cancer metastasis[35-37]. To our knowledge, no intrahepatic metastatic cancer model with a humanized liver has been available to date[25,30,35-37]. The m-liver in the present study was chimeric and was composed of normal h-hepatocytes and m-hepatocytes. Previous studies have reported that the h-hepatocytes in these chimeric livers are functional and secreted a variety of hepatic proteins, such as Alb, -1 antitrypsin, apolipoprotein A, apolipoprotein E, several clotting factors, and complement proteins present in h-plasma[38]. Transplanted h-hepatocytes also retain normal pharmacological responses, which makes the chimeric mouse model useful for studying the metabolism of compounds that cannot be easily administered to healthy volunteers[14,15]. *In vivo* studies using these mice showed their utility in evaluating the metabolism of drugs catalyzed by both phase I and phase II enzymes[13-15,39,40]. Since the liver functions of

the chimeric mice described in this study have not yet been characterized, future studies are needed to assess the model for anti-cancer drug testing. Taking together, the h-hepatocyte-chimeric mice may provide a useful bridge for studying human liver-related diseases because of the similarities with humans in physiological function and drug kinetics.

In conclusion, we have established a unique and novel animal model for studying liver cancer metastasis. The chimeric liver of the uPA/SCID mouse containing both human cancer cells and hepatocytes could be utilized as an appropriate model for *in vivo* testing of the efficacy and human-type metabolisms of candidate drugs for anti-cancer treatment as well as studying the mechanisms of liver cancer metastasis.

ACKNOWLEDGMENTS

COMMENTS

Background
One of the major target organs for cancer metastasis is the liver, and therefore, there has been increasing needs for animal models that can sufficiently mimic the pathophysiological situation in human liver and that are suitable for investigating the mechanisms of hepatic cancer metastasis.

Research frontiers
An ideal animal model for liver metastasis of human cancer cells should possess at least two key features. First, the transplanted cancer cells need to invade and colonize the liver of the host. Second, the liver of the host model has to provide the human cells with appropriate pathophysiological microenvironments that recapitulate the human liver *in vivo*. In the present study, the authors established a unique and novel animal model with both of these features.

Innovations and breakthroughs
A liver-humanized mouse was generated by transplanting healthy and normal h-hepatocytes into urokinase type plasminogen activator/severe combined immunodeficient (uPA/SCID) mice (immuno- and liver- compromized mice), and the liver was stably and reproducibly replaced with human hepatocytes. This is the first report of a novel experimental model that sufficiently mimics the pathophysiological situation of human liver.

Applications
The chimeric liver of the uPA/SCID mouse containing both human cancer cells and hepatocytes could be utilized as an appropriate model for the *in vivo* testing of anti-cancer drugs as well as studying the mechanisms of liver cancer metastasis.

Terminology
The uPA/SCID mouse is a transgenic mouse line that expressed uPA under the control of the albumin enhancer/promoter which constitutively damages the hepatocytes due to constant exposure to uPA. A liver- humanized mouse (chimeric mouse) was generated by transplanting healthy and normal human hepatocytes into mouse liver of the uPA/SCID mouse (immuno- and liver-compromized mouse), which had been generated by mating the uPA-Tg mouse with the SCID mouse. This mouse model sufficiently mimics the pathophysiological situation in human liver.

Peer review
This study tries to establish an animal model with h-hepatocyte-repopulated liver for *in vivo* study of liver cancer using uPA/SCID mouse, which could be useful for studying liver cancer metastasis. The authors transfected uPA/SCID mouse either with human gastric cancer cells (h-GCCs) or h-GCCs with h-hepatocytes and observed that both colonies can repopulate mouse liver. The study is well conducted, the manuscript is well-written and the figures are of good quality.

REFERENCES

1 **Yamamoto J**, Saiura A, Koga R, Seki M, Ueno M, Oya M, Azekura K, Seto Y, Ohyama S, Fukunaga S, Yamaguchi T, Kokudo N, Makuuchi M, Muto T. Surgical treatment for metastatic malignancies. Nonanatomical resection of liver metastasis: indications and outcomes. *Int J Clin Oncol* 2005; **10**: 97-102

2 **Ishizu K**, Sunose N, Yamazaki K, Tsuruo T, Sadahiro S, Makuuchi H, Yamori T. Development and characterization of a model of liver metastasis using human colon cancer HCT-116 cells. *Biol Pharm Bull* 2007; **30**: 1779-1783

3 **Leen E**, Ceccotti P, Moug SJ, Glen P, MacQuarrie J, Angerson WJ, Albrecht T, Hohmann J, Oldenburg A, Ritz JP, Horgan PG. Potential value of contrast-enhanced intraoperative ultrasonography during partial hepatectomy for metastases: an essential investigation before resection? *Ann Surg* 2006; **243**: 236-240

4 **Giavazzi R**, Campbell DE, Jessup JM, Cleary K, Fidler IJ. Metastatic behavior of tumor cells isolated from primary and metastatic human colorectal carcinomas implanted into different sites in nude mice. *Cancer Res* 1986; **46**: 1928-1933

5 **Takamura M**, Sakamoto M, Genda T, Ichida T, Asakura H, Hirohashi S. Inhibition of intrahepatic metastasis of human hepatocellular carcinoma by Rho-associated protein kinase inhibitor Y-27632. *Hepatology* 2001; **33**: 577-581

6 **Niedergethmann M**, Alves F, Neff JK, Heidrich B, Aramin N, Li L, Pilarsky C, Grützmann R, Allgayer H, Post S, Gretz N. Gene expression profiling of liver metastases and tumour invasion in pancreatic cancer using an orthotopic SCID mouse model. *Br J Cancer* 2007; **97**: 1432-1440

7 **Bosma GC**, Custer RP, Bosma MJ. A severe combined immunodeficiency mutation in the mouse. *Nature* 1983; **301**: 527-530

8 **Suemizu H**, Hasegawa M, Kawai K, Taniguchi K, Monnai M, Wakui M, Suematsu M, Ito M, Peltz G, Nakamura M. Establishment of a humanized model of liver using NOD/Shi-scid IL2Rgnull mice. *Biochem Biophys Res Commun* 2008; **377**: 248-252

9 **Suemizu H**, Monnai M, Ohnishi Y, Ito M, Tamaoki N, Nakamura M. Identification of a key molecular regulator of liver metastasis in human pancreatic carcinoma using a novel quantitative model of metastasis in NOD/SCID/gammacnull (NOG) mice. *Int J Oncol* 2007; **31**: 741-751

10 **Heckel JL**, Sandgren EP, Degen JL, Palmiter RD, Brinster RL. Neonatal bleeding in transgenic mice expressing urokinase-type plasminogen activator. *Cell* 1990; **62**: 447-456

11 **Mercer DF**, Schiller DE, Elliott JF, Douglas DN, Hao C, Rinfret A, Addison WR, Fischer KP, Churchill TA, Lakey JR, Tyrrell DL, Kneteman NM. Hepatitis C virus replication in mice with chimeric human livers. *Nat Med* 2001; **7**: 927-933

12 **Tateno C**, Yoshizane Y, Saito N, Kataoka M, Utoh R, Yamasaki C, Tachibana A, Soeno Y, Asahina K, Hino H, Asahara T, Yokoi T, Furukawa T, Yoshizato K. Near completely humanized liver in mice shows human-type metabolic responses to drugs. *Am J Pathol* 2004; **165**: 901-912

13 **Utoh R**, Tateno C, Yamasaki C, Hiraga N, Kataoka M, Shimada T, Chayama K, Yoshizato K. Susceptibility of chimeric mice with livers repopulated by serially subcultured human hepatocytes to hepatitis B virus. *Hepatology* 2008; **47**: 435-446

14 **Yoshizato K**, Tateno C. A human hepatocyte-bearing mouse: an animal model to predict drug metabolism and effectiveness in humans. *PPAR Res* 2009; **2009**: 476217

15 **Yoshizato K**, Tateno C. In vivo modeling of human liver for pharmacological study using humanized mouse. *Expert Opin Drug Metab Toxicol* 2009; **5**: 1435-1446

16 **Chang YC**, Nagasue N, Abe S, Taniura H, Kumar DD, Nakamura T. Comparison between the clinicopathologic features of AFP-positive and AFP-negative gastric cancers. *Am J Gastroenterol* 1992; **87**: 321-325

17   **Sekiguchi M**, Fujii Y, Saito A, Suzuki T, Shiroko Y, Naka-mura H, Hasumi K. Alpha-fetoprotein-producing gastric carcinoma: biological properties of a cultured cell line. *J Gastroenterol* 1995; **30**: 589-598

18   **Kamata S**, Kishimoto T, Kobayashi S, Miyazaki M, Ishikura H. Possible involvement of persistent activity of the mam-malian target of rapamycin pathway in the cisplatin resis-tance of AFP-producing gastric cancer cells. *Cancer Biol Ther* 2007; **6**: 1036-1043

19   **Amemiya H**, Kono K, Mori Y, Takahashi A, Ichihara F, Iizu-ka H, Sekikawa T, Matsumoto Y. High frequency of c-Met expression in gastric cancers producing alpha- fetoprotein. *Oncology* 2000; **59**: 145-151

20   **Shanmukhappa K**, Matte U, Degen JL, Bezerra JA. Plasmin-mediated proteolysis is required for hepatocyte growth factor activation during liver repair. *J Biol Chem* 2009; **284**: 12917-12923

21   **Sandgren EP**, Palmiter RD, Heckel JL, Daugherty CC, Brinster RL, Degen JL. Complete hepatic regeneration after somatic deletion of an albumin-plasminogen activator trans-gene. *Cell* 1991; **66**: 245-256

22   **Van Buren G**, Gray MJ, Dallas NA, Xia L, Lim SJ, Fan F, Mazar AP, Ellis LM. Targeting the urokinase plasminogen activator receptor with a monoclonal antibody impairs the growth of human colorectal cancer in the liver. *Cancer* 2009; **115**: 3360-3368

23   **Madsen MA**, Deryugina EI, Niessen S, Cravatt BF, Quigley JP. Activity-based protein profiling implicates urokinase ac-tivation as a key step in human fibrosarcoma intravasation. *J Biol Chem* 2006; **281**: 15997-16005

24   **Obermajer N**, Doljak B, Kos J. Cytokeratin 8 ectoplasmic domain binds urokinase-type plasminogen activator to breast tumor cells and modulates their adhesion, growth and invasiveness. *Mol Cancer* 2009; **8**: 88

25   **Desdouets C**, Fabre M, Gauthier F, Bréchot C, Sobczak-Thépot J. Proliferation and differentiation of a human hepa-toblastoma transplanted in the Nude mouse. *J Hepatol* 1995; **23**: 569-577

26   **Leveille-Webster CR**, Arias IA. Establishment and serial quantification of intrahepatic xenografts of human hepato-cellular carcinoma in severe combined immunodeficiency mice, and development of therapeutic strategies to over-come multidrug resistance. *Clin Cancer Res* 1996; **2**: 695-706

27   **Miyoshi E**, Noda K, Ko JH, Ekuni A, Kitada T, Uozumi N, Ikeda Y, Matsuura N, Sasaki Y, Hayashi N, Hori M, Taniguchi N. Overexpression of alpha1-6 fucosyltransferase in hep-atoma cells suppresses intrahepatic metastasis after splenic injection in athymic mice. *Cancer Res* 1999; **59**: 2237-2243

28   **Kollmar O**, Schilling MK, Menger MD. Experimental liver metastasis: standards for local cell implantation to study isolated tumor growth in mice. *Clin Exp Metastasis* 2004; **21**: 453-460

29   **Hardy B**, Morgenstern S, Raiter A, Rodionov G, Fadaeev L, Niv Y. BAT monoclonal antibody immunotherapy of human metastatic colorectal carcinoma in mice. *Cancer Lett* 2005; **229**: 217-222

30   **Schnater JM**, Bruder E, Bertschin S, Woodtli T, de Theije C, Pietsch T, Aronson DC, von Schweinitz D, Lamers WH, Köhler ES. Subcutaneous and intrahepatic growth of human hepatoblastoma in immunodeficient mice. *J Hepatol* 2006; **45**: 377-386

31   **Meuleman P**, Leroux-Roels G. The human liver-uPA-SCID mouse: a model for the evaluation of antiviral compounds against HBV and HCV. *Antiviral Res* 2008; **80**: 231-238

32   **Kato R**. Characteristics and differences in the hepatic mixed function oxidases of different species. *Pharmacol Ther* 1979; **6**: 41-98

33   **Green CE**, LeValley SE, Tyson CA. Comparison of amphet-amine metabolism using isolated hepatocytes from five species including human. *J Pharmacol Exp Ther* 1986; **237**: 931-936

34   **Naritomi Y**, Terashita S, Kimura S, Suzuki A, Kagayama A, Sugiyama Y. Prediction of human hepatic clearance from in vivo animal experiments and in vitro metabolic studies with liver microsomes from animals and humans. *Drug Metab Dispos* 2001; **29**: 1316-1324

35   **Hata Y**, Uchino J, Sato K, Sasaki F, Une Y, Naito H, Manabe K, Kuwahara T, Kasai Y. Establishment of an experimental model of human hepatoblastoma. *Cancer* 1982; **50**: 97-101

36   **Fuchs J**, Wenderoth M, von Schweinitz D, Haindl J, Leus-chner I. Comparative activity of cisplatin, ifosfamide, doxo-rubicin, carboplatin, and etoposide in heterotransplanted hepatoblastoma. *Cancer* 1998; **83**: 2400-2407

37   **Kneteman NM**, Mercer DF. Mice with chimeric human liv-ers: who says supermodels have to be tall? *Hepatology* 2005; **41**: 703-706

38   **Meuleman P**, Libbrecht L, De Vos R, de Hemptinne B, Ge-vaert K, Vandekerckhove J, Roskams T, Leroux-Roels G. Morphological and biochemical characterization of a human liver in a uPA-SCID mouse chimera. *Hepatology* 2005; **41**: 847-856

39   **Katoh M**, Tateno C, Yoshizato K, Yokoi T. Chimeric mice with humanized liver. *Toxicology* 2008; **246**: 9-17

40   **Tsuge M**, Hiraga N, Takaishi H, Noguchi C, Oga H, Imam-ura M, Takahashi S, Iwao E, Fujimoto Y, Ochi H, Chayama K, Tateno C, Yoshizato K. Infection of human hepatocyte chi-meric mouse with genetically engineered hepatitis B virus. *Hepatology* 2005; **42**: 1046-1054

Fibrogenesis & Tissue Repair

RESEARCH   **Open Access**

Induction of microRNA-214-5p in human and rodent liver fibrosis

Masashi Iizuka[1,3], Tomohiro Ogawa[1,2,3], Masaru Enomoto[1,3], Hiroyuki Motoyama[1,3], Katsutoshi Yoshizato[1,3], Kazuo Ikeda[4,3] and Norifumi Kawada[1,3*]

Abstract

Background: miRNAs are non-coding RNAs that regulate gene expression in a wide range of biological contexts, including a variety of diseases. The present study clarified the role of miR-214-5p in hepatic fibrogenesis using human clinical tissue samples, livers from rodent models, and cultured hepatic stellate cells.

Methods: The expression of miR-214-5p and genes that are involved in liver fibrosis were analyzed in hepatitis C virus-infected human livers, rodent fibrotic livers, a human stellate cell line (LX-2), and the cells from intact mouse livers using real-time PCR. The effect of miR-214-5p overexpression in LX-2 cells on cell function was investigated. Twist-1 expression in the liver tissues of mouse models and primary-cultured stellate cells was also analyzed.

Results: miR-214-5p was upregulated in human and mouse livers in a fibrosis progression–dependent manner. miR-214-5p expression increased during the culture-dependent activation of mouse primary stellate cells and was significantly higher in stellate cells than in hepatocytes. The overexpression of miR-214-5p in LX-2 cells increased the expression of fibrosis-related genes, such as matrix metalloproteinase (MMP)-2, MMP-9, α-smooth muscle actin, and transforming growth factor (TGF)-β1. TGF-β stimulation induced miR-214-5p in LX-2 cells. Twist-1 was increased in fibrotic mouse livers and induced during mouse stellate cell activation.

Conclusion: miR-214-5p may play crucial roles in the activation of stellate cells and the progression of liver fibrosis. Twist-1 may regulate miR-214-5p expression in the liver, particularly in stellate cells.

Keywords: Collagen, Hepatocyte, Non-coding RNA, Stellate cell, Transforming growth factor-β

Background

Liver fibrosis is a consequence of chronic liver trauma caused by hepatitis B or hepatitis C virus (HCV) infection, alcohol abuse, or steatohepatitis, which ultimately leads to liver cirrhosis, liver failure, and hepatocellular carcinoma [1]. Liver fibrosis is characterized by an abnormal accumulation of extracellular matrix (ECM) components, including types I and III collagen, laminin, and proteoglycans, in the liver parenchyma [2,3]. Transforming growth factor (TGF)-β, which is produced and released by activated macrophages and platelets at the site of local inflammation, is considered to play a primary role in the fibrotic process [3]. Hepatic stellate cells - which are localized in

Disse's space, store vitamin A and act as tissue-specific pericytes under physiological conditions - undergo activation and transformation into myofibroblast-like cells that express α-smooth muscle actin (α-SMA) during persistent inflammation. The activated stellate cells become an additional source of TGF-β and a principal producer of ECM components. However, the detailed molecular mechanisms of TGF-β production in these cells have not been determined [4].

miRNAs are 20 to 24 nucleotide non-coding RNAs that are involved in the post-transcriptional regulation of gene expression. Mature miRNAs are incorporated into an RNA-induced silencing complex that recognizes target mRNAs through imperfect base pairing with the miRNA. This action triggers the translational inhibition or destabilization of the target mRNA, which results in the regulation of crucial biological processes, such as development, differentiation, apoptosis and cellular proliferation
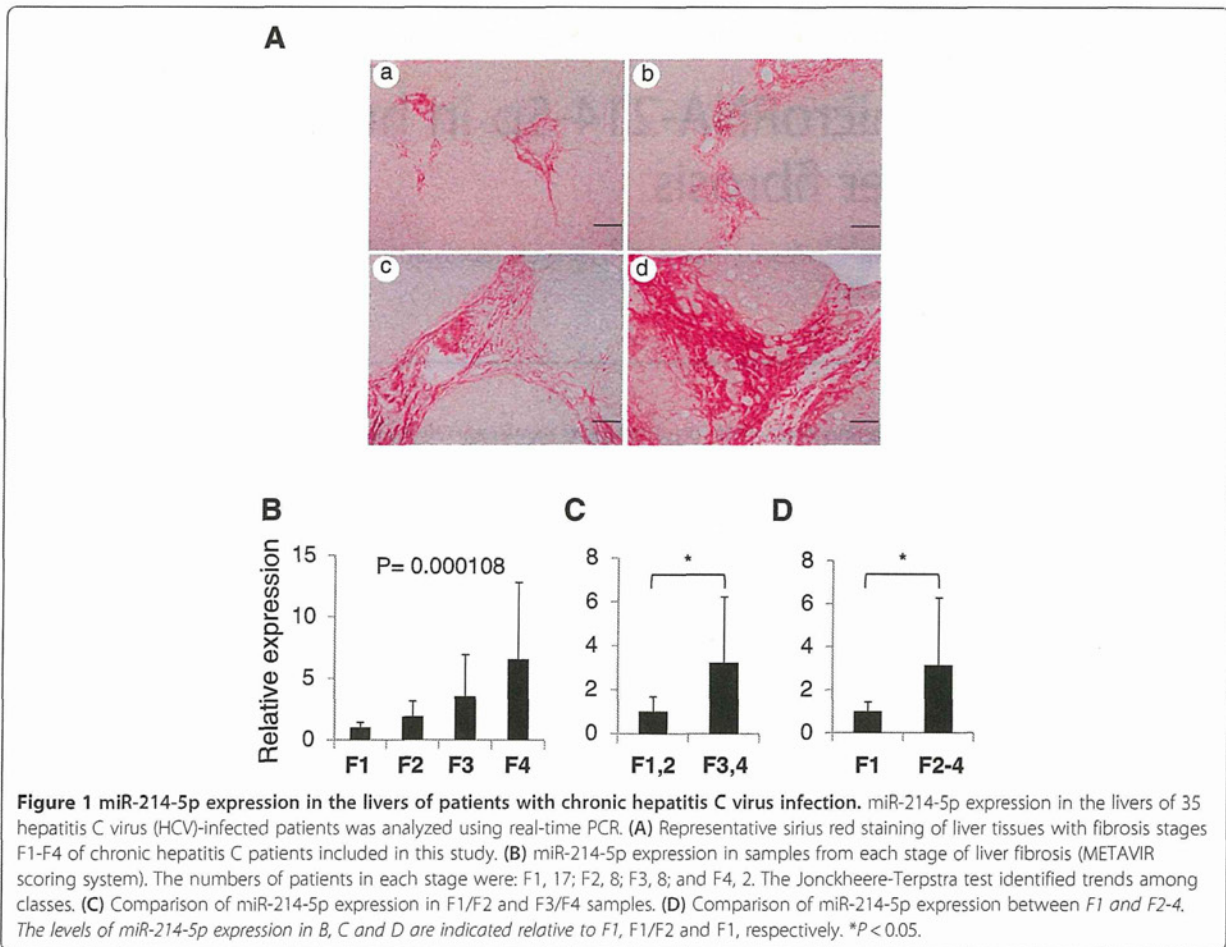
* Correspondence: kawadanori@med.osaka-cu.ac.jp
[1]Department of Hepatology, Graduate School of Medicine, Osaka City University, 1-4-3, Asahimachi, Abeno, Osaka 545-8585, Japan
[3]PhoenixBio Co. Ltd., Hiroshima, Japan, 3-4-1, Kagamiyama, Higashi-Hiroshima City, Hiroshima 739-0046, Japan
Full list of author information is available at the end of the article

Figure 1 miR-214-5p expression in the livers of patients with chronic hepatitis C virus infection. miR-214-5p expression in the livers of 35 hepatitis C virus (HCV)-infected patients was analyzed using real-time PCR. **(A)** Representative sirius red staining of liver tissues with fibrosis stages F1-F4 of chronic hepatitis C patients included in this study. **(B)** miR-214-5p expression in samples from each stage of liver fibrosis (METAVIR scoring system). The numbers of patients in each stage were: F1, 17; F2, 8; F3, 8; and F4, 2. The Jonckheere-Terpstra test identified trends among classes. **(C)** Comparison of miR-214-5p expression in F1/F2 and F3/F4 samples. **(D)** Comparison of miR-214-5p expression between *F1 and F2-4*. *The levels of miR-214-5p expression in B, C and D are indicated relative to F1, F1/F2 and F1, respectively. *$P < 0.05$.

[5,6]. Aberrant expression of miRNAs in tissues correlates with a variety of diseases, including proliferative vascular disease [7], cardiac disorders [8,9], polycystic kidney disease [10], and cancer [11,12]. Several miRNAs can be used as biomarkers for cancer [13,14] because miRNA expression patterns in human cancer are tissue specific [15].

miR-122 is the most abundant miRNA in the liver, where it regulates fat metabolism and the replication of HCV in hepatocytes and contributes to carcinogenesis [16,17]. miR-122 has been used as a novel biomarker for liver damage in rat models of hepatocellular injury caused by a methionine- and choline-deficient diet (MCDD), CCl_4 or acetaminophen and bile duct ligation [18]. We previously reported that miR-29b regulates collagen expression by binding to the 3′-UTR of the type 1 collagen alpha 1 chain (Col1a1) and SP1 mRNAs [19], and miR-29b directly inhibits the activation of mouse stellate cells in primary culture [20]. It was recently reported that miR-19b suppresses the activation of stellate cells via the inhibition of TGF-β signaling by interacting with the type II TGF-β receptor [21].

miR-214-5p is a product of the 110 bp *miR-214* gene in the intron of the *Dynamin-3* gene on human Chromosome 1-NC_000001.10, which produces a mature miRNA with a sequence of ugccugucuacacuugcugugc [22]. TGF-β induces miR-214 expression in rat tubular epithelial cells and mesangial cells [23], and miR-214 interacts with Quaking to inhibit angiogenesis [24]. However, the pathophysiological roles of miR-214 remain largely unknown. Here, we report the upregulation of miR-214-5p in a fibrosis progression–dependent manner in HCV-infected human livers and in the livers of a rodent fibrosis model. The role of miR-214-5p in hepatic stellate cell activation is also discussed.

Results
miR-214 expression in chronic hepatitis C patients
We previously found that, using microRNA array analysis, miR-221/222 expression was upregulated in a fibrosis progression–dependent manner in human livers that are chronically infected with HCV [25]. In addition, we quantitatively confirmed the miR-214-5p expression
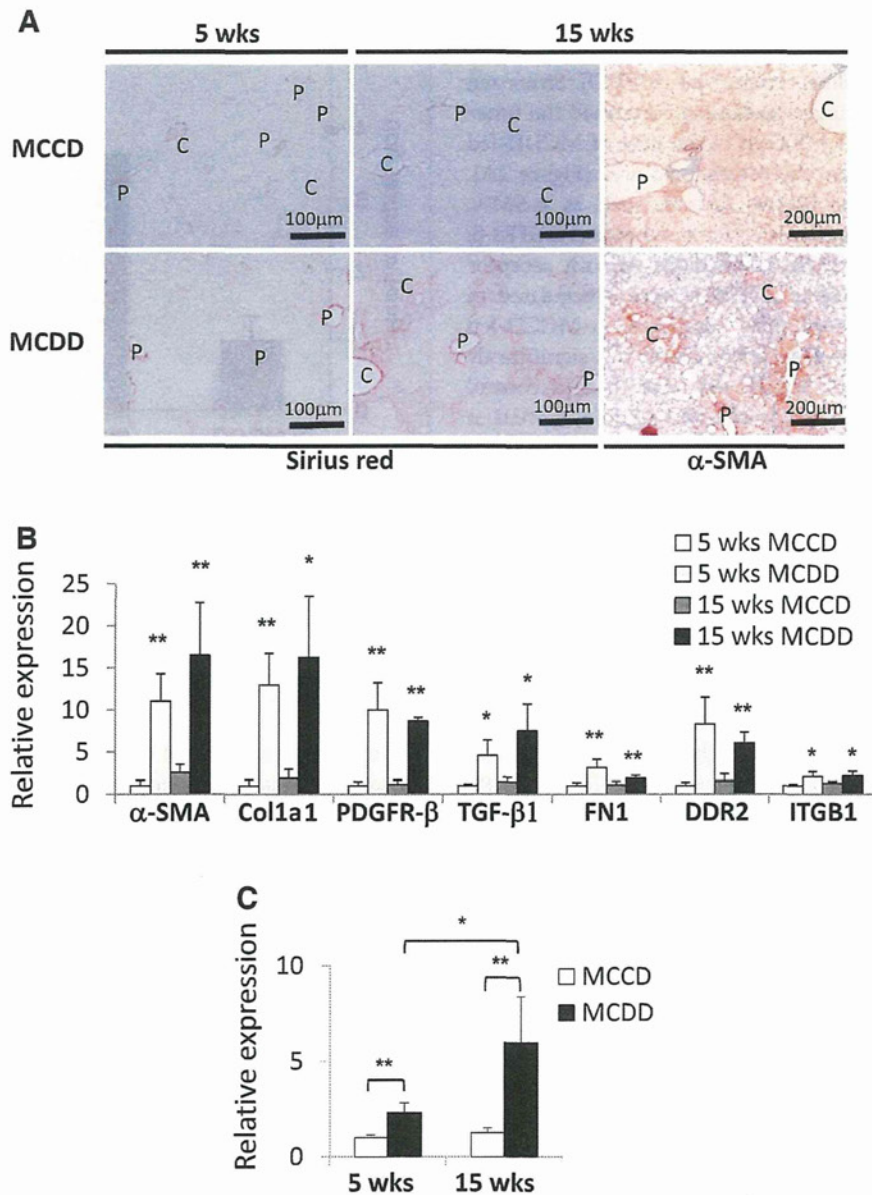
Figure 2 miR-214-5p expression in mouse livers with fibrosis induced by an methionine- and choline-deficient diet. (A) Sirius red staining (left and middle panels) and α-smooth muscle actin (SMA) immunostaining (right panels) of mouse liver tissues. Collagen deposition and an increase in α-SMA-positive cells were evident around the central vein area of the liver of mice that received the MCDD for 15 weeks. Scale bars, 100 μm (left and middle panels) and 200 μm (right panels). P, portal vein. C, central vein. **(B)** The mRNA expression of α-smooth muscle actin (α-SMA), the type 1 collagen alpha 1 chain (Col1a1), platelet-derived growth factor receptor (PDGFR)-β, transforming growth factor (TGF)-β1, fibronectin (FN)1, discoidin domain receptor (DDR)2, and β1 integrin (ITGB1) in fibrotic mouse livers was analyzed using real-time PCR. The results are expressed relative to mRNA expression at 5 weeks of the methionine- and choline-control diet (MCCD). *$P < 0.05$. **$P < 0.01$. **(C)** miR-214-5p expression in fibrotic mouse livers was analyzed using real-time PCR. The results are expressed relative to the expression of miR-214-5p at 5 weeks of the MCCD. *$P < 0.05$. **$P < 0.01$.

levels in 35 HCV patients with individual stages of liver fibrosis (Figure 1A) using real-time PCR. We found that miR-214-5p expression increased according to the stage of fibrosis ($P = 0.000108$) (Figure 1B) and was significantly higher in patients with advanced liver fibrosis than in those with mild fibrosis (F1/F2 versus F3/F4: 3.2-fold, $P < 0.05$; F1 versus F2-4: 3.1-fold, $P < 0.05$) (Figure 1C,D).

miR-214 expression in a mouse model of liver fibrosis

Liver fibrosis was induced by feeding mice a MCDD for 5 or 15 weeks and then compared with mice fed a methionine- and choline-control diet (MCCD). Sirius red staining and α-SMA immunostaining confirmed the time-dependent induction of fibrosis in the liver of MCDD-fed mice, especially around the central vein area (Figure 2A). The mRNAs of liver fibrosis factors, such as α-SMA, Col1a1, platelet-derived growth factor receptor (PDGFR)-β, TGF-β1, fibronectin (FN) 1, discoidin domain receptor (DDR) 2, and β1 integrin (ITGB1), were upregulated in the livers of MCDD-fed mice compared to MCCD-fed mice (Figure 2B). miR-214-5p expression was significantly higher in the livers of MCDD-fed mice than in control mice (2.1-fold, $P < 0.01$ at 5 weeks; and 4.8-fold, $P < 0.01$ at 15 weeks) (Figure 2C).

miR-214 expression in a rat resolution model of liver fibrosis

We previously demonstrated the resolution of liver fibrosis with steatohepatitis in a rat model induced by giving MCDD; that is, rats received either MCCD for 10 weeks, MCDD for 10 weeks, or MCDD for 8 weeks followed by MCCD for the last 2 weeks (the last of the these being the recovery group) [26]. miR-214-5p expression was significantly greater in the livers of rats that received MCDD for 10 weeks than in those that received MCCD for 10 weeks. However, these levels returned to control levels in the livers of rats that received the MCDD diet for 8 weeks followed by the MCCD diet for 2 weeks, consistent with recovery from the fibrosis (Figure 3). These results clearly suggest a close correlation between miR-214-5p expression in the liver, fibrosis development, and fibrosis-related mRNA expression.

miR-214-5p expression in hepatic stellate cells

We assessed the contribution of activated hepatic stellate cells to the increase in miR-214-5p in fibrotic mouse livers. miR-214-5p expression increased during the culture-dependent activation process in mouse stellate cells (2.7-fold increase at day 7 compared to day 1, $P < 0.05$) (Figure 4A). As expected, the induction of miR-214-5p was accompanied by an increase in the expression of α-SMA, Col1a1, PDGFR-β, and FN1 mRNA (Figure 4B). In addition, miR-214-5p expression was markedly higher in LX-2, a widely used human hepatic stellate cell line, than in human liver cancer cell lines such as HepG2 and Huh7 (108- and 39-fold, respectively) (Figure 4C).

We next isolated individual hepatocytes, non-parenchymal cells, and hepatic stellate cells from intact mouse livers to verify the cellular source of miR-214-5p. miR-214-5p was localized to non-parenchymal cells and hepatic stellate cells but expressed at negligible levels in hepatocytes (Figure 4D). These results suggest that miR-
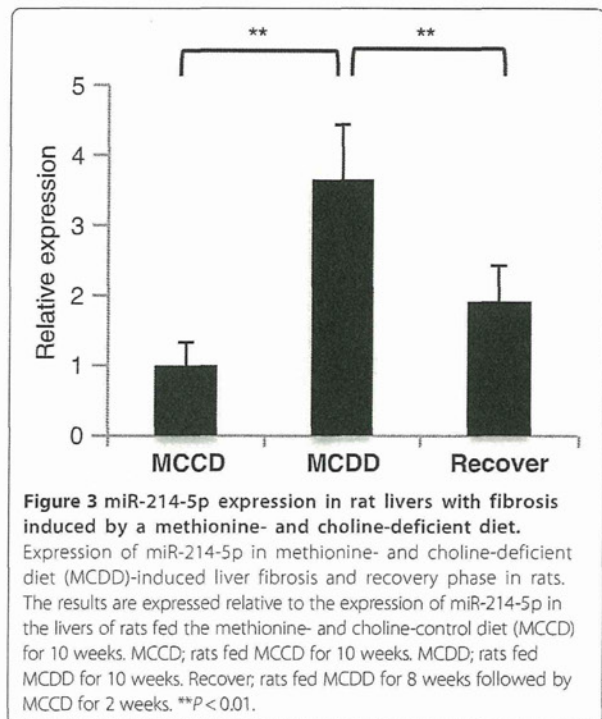
Figure 3 miR-214-5p expression in rat livers with fibrosis induced by a methionine- and choline-deficient diet. Expression of miR-214-5p in methionine- and choline-deficient diet (MCDD)-induced liver fibrosis and recovery phase in rats. The results are expressed relative to the expression of miR-214-5p in the livers of rats fed the methionine- and choline-control diet (MCCD) for 10 weeks. MCCD; rats fed MCCD for 10 weeks. MCDD; rats fed MCDD for 10 weeks. Recover; rats fed MCDD for 8 weeks followed by MCCD for 2 weeks. **$P < 0.01$.
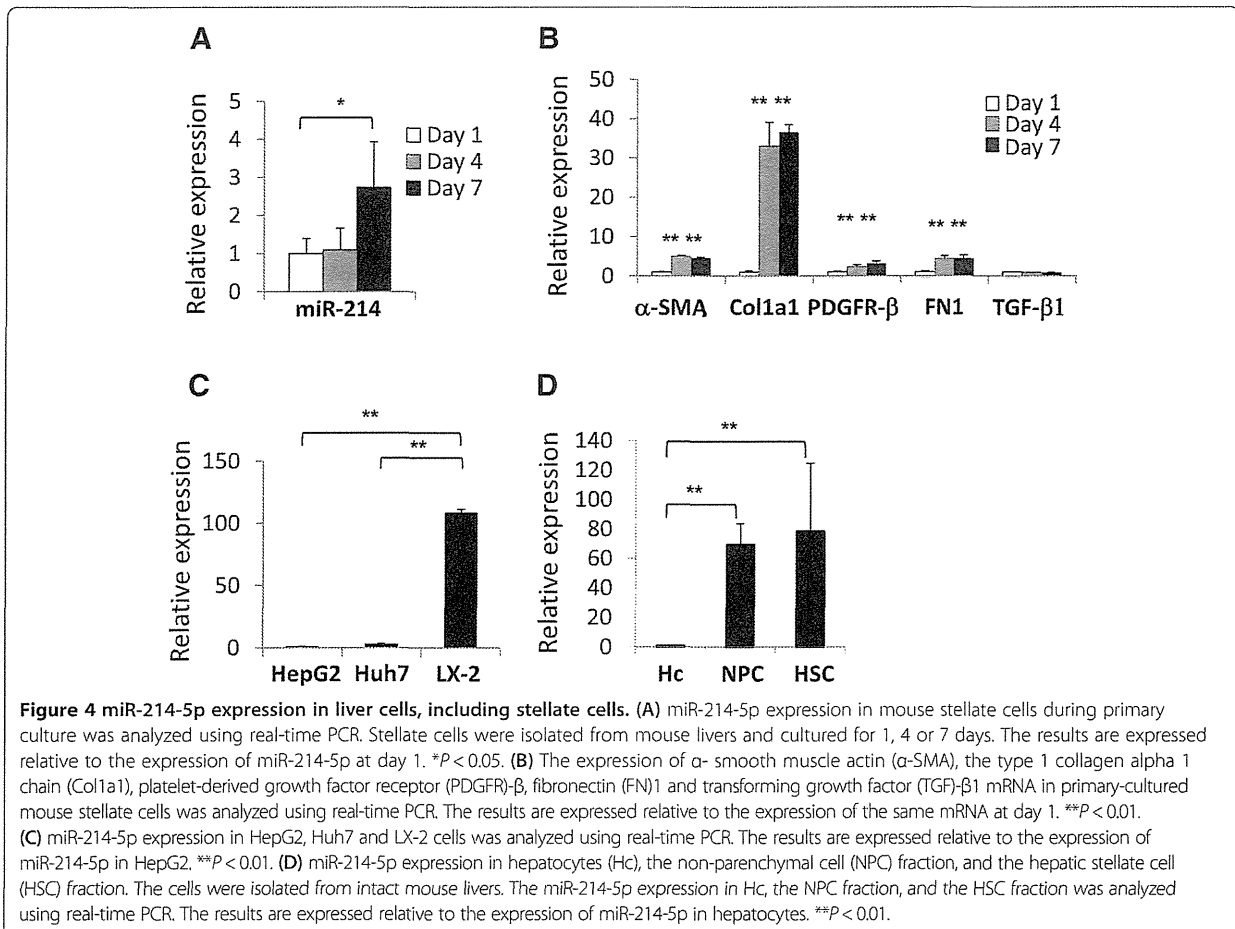
214 induction in fibrotic livers reflects the number and activation status of hepatic stellate cells.

The effect of miR-214 overexpression on gene expression in stellate cells

We investigated the effect of miR-214-5p overexpression on fibrosis-related gene expression in stellate cells to clarify the role of this miRNA in stellate cell activation. miR-214-5p was overexpressed in LX-2 cells by transfection with an miR-214 precursor. The overexpression of miR-214 significantly increased the expression of matrix metalloproteinase-2 (MMP-2), MMP-9, α-SMA, and TGF-β1 compared to cells transfected with control microRNA (1.7-, 2.8-, 1.7- and 2.0-fold, respectively; $P < 0.01$) (Figure 5). These results indicate the strong participation of miR-214 in the activation of stellate cells.

Induction of miR-214 expression by TGF-β1

TGF-β_1 induces miR-214 expression in rat tubular epithelial cells and mesangial cells [23]. TGF-β_1 is essential for hepatic stellate cell activation. We assessed the stimulatory effect of TGF-β on miR-214-5p expression in LX-2 cells. TGF-β_1 (3 and 10 ng/ml) significantly stimulated miR-214-5p expression in LX-2 cells after 24 hours (1.75-fold, $P < 0.05$)(Figure 6A). In contrast, the expression of the miR-214/199a cluster is controlled by the transcription factor Twist-1 [22]. Real-time PCR analysis revealed that Twist-1 expression increased in the livers of mice that received MCDD compared to those of MCCD-fed mice

Figure 4 miR-214-5p expression in liver cells, including stellate cells. (A) miR-214-5p expression in mouse stellate cells during primary culture was analyzed using real-time PCR. Stellate cells were isolated from mouse livers and cultured for 1, 4 or 7 days. The results are expressed relative to the expression of miR-214-5p at day 1. *$P < 0.05$. **(B)** The expression of α- smooth muscle actin (α-SMA), the type 1 collagen alpha 1 chain (Col1a1), platelet-derived growth factor receptor (PDGFR)-β, fibronectin (FN)1 and transforming growth factor (TGF)-β1 mRNA in primary-cultured mouse stellate cells was analyzed using real-time PCR. The results are expressed relative to the expression of the same mRNA at day 1. **$P < 0.01$. **(C)** miR-214-5p expression in HepG2, Huh7 and LX-2 cells was analyzed using real-time PCR. The results are expressed relative to the expression of miR-214-5p in HepG2. **$P < 0.01$. **(D)** miR-214-5p expression in hepatocytes (Hc), the non-parenchymal cell (NPC) fraction, and the hepatic stellate cell (HSC) fraction. The cells were isolated from intact mouse livers. The miR-214-5p expression in Hc, the NPC fraction, and the HSC fraction was analyzed using real-time PCR. The results are expressed relative to the expression of miR-214-5p in hepatocytes. **$P < 0.01$.

(2.2-fold at 5 weeks, $P < 0.05$; and 3.6-fold at 15 weeks, $P < 0.05$) (Figure 6B). Twist-1 mRNA expression was also induced in a time-dependent manner after culture initiation in primary-cultured mouse stellate cells (Figure 6C).

Discussion

This is the first report to show that miR-214-5p is involved in organ fibrogenesis, specifically in the liver. miR-214 has previously been predicted to be a key molecule in proliferation in breast [27] and ovarian cancer cells [28], tumor progression in melanoma [29], and growth in HeLa cells [30]. miR-214 and miR-199a are encoded in a region that contains an E-box DNA promoter sequence [22]. A transcription factor, Twist-1, binds to the E-box region, regulating miR-214 and miR-199a expression [22]. The present study showed that miR-214 expression is upregulated in a fibrosis progression-dependent manner in the livers of patients with chronic HCV infection and in mice with diet-induced steatohepatitis (Figures 1 and 2). We previously reported an increase in miR-199a in the fibrotic livers of patients with chronic HCV infection [25], and similar findings have been reported by others [31-33]. These data and the upregulation

of Twist-1 in MCDD-induced mouse liver fibrosis (Figure 4) suggest that Twist-1 controls the expression of the miR-214/199a cluster in the liver. Further studies will be needed to clarify the possible involvement of Twist-1 in the expression of miR-214-5p in LX-2 cells.

The present study revealed that miR-214-5p overexpression in LX-2 cells significantly increased MMP-2, MMP-9, α-SMA, and TGF-β1 mRNA expression. The overexpression of miR-199a in LX-2 cells triggers the upregulation of tissue inhibitor of metalloproteinase (TIMP)-1, Col1a1, and MMP-13 mRNA [34]. These results suggest that the miR-214/199a cluster plays a primary role in stellate cell activation. However, an understanding of the precise molecular events involved requires further research.

Conversely, the overexpression of miR-214-5p in LX-2 cells did not alter the expression of MAPK/Erk kinase 3 (MEK3), transcription factor AP-2 gamma (TFAP2C) [29], Plenxin-B1 [30], c-Jun N-terminal kinase 1 (Jnk1) [34], phosphatase and tensin homolog (PTEN) [35], enhancer of zeste homolog 2 (Ezh2) [36], and Quaking mRNA [24], which had been reported to be targets of miR-214 (MEK3: 0.72- to 0.77-fold, Jnk1: 1.05- to 1.20-fold,